Apoptosis-associated speck-like protein containing CARD forms specks but does not activate caspase-1 in the absence of NLRP3 during macrophage swelling

Vincent Compan*,§, Fátima Martín-Sánchez†, Alberto Baroja-Mazo†, Gloria López-Castejón*, Ana I. Gomez†, Alexei Verkhratsky*, David Brough* & Pablo Pelegrín*,†

*Faculty of Life Sciences, University of Manchester, Manchester M13 9PT, UK

†Inflammation and Experimental Surgery Unit, CIBERehd, Murcia's BioHealth Research Institute IMIB-Arrixaca, Clinical University Hospital "Virgen de la Arrixaca", 30120 Murcia, Spain.

Running Title: ASC speck formation during cell swelling

Total length of the sections "Introduction", "Material & Methods", "Results" and "Discussion": 5,937 words

ABSTRACT

Apoptosis-associated speck-like protein containing a CARD (ASC) is a key adaptor molecule required for inflammatory processes. ASC acts by bridging NLRP proteins, such as NLRP3, with pro-caspase-1 within the inflammasome complex that subsequently results in the activation of caspase-1 and the secretion of interleukin (IL)-1β and IL-18. In response to bacterial infection, ASC also forms specks by self-oligomerization to activate caspase-1 and induce pyroptosis. Hitherto the role of these specks in NLRP3 inflammasome activation in response to danger signals is largely unexplored. Here we report that under hypotonic conditions, ASC formed specks independently of NLRP3 that did not activate caspase-1. These specks were not associated with pyroptosis and were controlled by Transient Receptor Potential Vanilloid 2 channel mediated signaling. However, interaction with NLRP3 enhanced ASC speck formation leading to fully functional inflammasomes and caspase-1 activation. This study reveals that the ASC speck could present different oligomerization assemblies and represents an essential step in the activation of functional NLRP3 inflammasomes.

INTRODUCTION

Inflammation is a response against infection, which is initiated by the activation of pattern-recognition receptors (PRRs) on macrophages. PRRs are triggered by both pathogen- and danger-associated molecular patterns (PAMPs and DAMPs, respectively), resulting in the production of proinflammatory cytokines (1). Signaling through PRRs of the Toll-like receptor family induces synthesis of the inactive forms of interleukin (IL)-1β and IL-18, two key proinflammatory cytokines that depend upon the activity of caspase-1 for their maturation and secretion.

The adaptor molecule apoptosis-associated speck-like protein containing a CARD (ASC or Pycard) is essential for caspase-1 activation in response to diverse disease and pathogen associated signals (2). ASC is a cytosolic protein that contains a C-terminal caspase recruitment domain (CARD) and an N-terminal pyrin (PYD) domain. ASC can control the activation of caspase-1 by two mechanisms: (*i*) as a molecular adaptor between PYD and CARD-containing signaling molecules within the inflammasome, a cytosolic PRR multiprotein complex; or (*ii*) via the oligomerization of ASC monomers into a cytosolic speck called the pyroptosome (2, 3). The pyroptosome is responsible for a specific type of cell death called pyroptosis, a mechanism mediated by caspase-1 activation through which macrophages infected with intracellular pathogens rapidly die facilitating pathogen clearance (4).

According to the current model for inflammasome activation, conformational changes in cytosolic PRRs of the Nucleotide binding and Leucine rich repeat Receptors (NLR) family leads to an interaction with caspase-1 (2). ASC is suggested to be necessary in bridging NLRP3 or AIM2 with pro-caspase-1 to form an inflammasome. In

this situation, ASC has been found to self-assemble into fiber-like structures from oligomers of NLRP3 or AIM2 culminating with the production of large protein aggregates that amplifies the activation of caspase-1 (5, 6). Other NLRs such as NLRC4 and NLRP1 can interact directly with caspase-1 through their CARD domains. However, recent studies have revealed that ASC is also necessary for caspase-1 activation within NLRC4 and NLRP1 complexes (7-10). In these situations ASC assembles into a ring-like structure surrounding NLRC4 oligomers (11). These data suggest that ASC is essential for inflammasome activity in general and that ASC could present different oligomerization assemblies.

The NLRP3-inflammasome is activated by diverse DAMPs and PAMPs. Its activation by DAMPs is central for 'sterile' inflammatory responses and for amplification of infection-induced inflammation (2). Endogenous DAMPs activating NLRP3 can be classified into two main categories: (*i*) 'soluble' activators, such as extracellular ATP acting through P2X7 receptors, or a decrease of extracellular osmolarity sensed by Transient Receptor Potential (TRP) channels; or (*ii*) 'particulate' crystalline factors, such as monosodium urate or cholesterol crystals (12-15). We have recently reported that the NLRP3 inflammasome adopts an inactive pre-assembled conformation that changes into an active form following variation in the intracellular potassium ion concentration (15). ASC is required for NLRP3 induced caspase-1 activation in response to extracellular hypotonicity and compacts pre-assembled NLRP3 complexes, accelerating their conformational change upon activation (15).

ASC represents an important target for the negative regulation of the inflammasome by endogenous proteins. Inflammasome dominant negative regulators

function by binding to ASC through the PYD or CARD domain inhibiting ASC-dependent processes (16). ASC may also be a target for drugs blocking IL-1β release, such as the cytokine release inhibitory drug 3 (CRID3), which targets ASC oligomerization during NLRP3 inflammasome activation (17, 18). Furthermore, ASC plays a key role in the development of different 'sterile' inflammatory responses involving the NLRP3 inflammasome, including gout, type 2 diabetes, atherosclerosis, metabolic syndrome, chronic obstructive pulmonary disease, spinal cord injury or Alzheimer's disease (12, 13, 19-23).

Although ASC is accepted to be critical for inflammasome activation, the different oligomerization states of ASC during inflammasome activation and its real time assembly kinetics with NLRP3 have not been addressed. Here, we studied ASC oligomerization and speck formation in response to hypotonicity and other NLRP3 activators, and the relationship between ASC speck formation and the activation of caspase-1. We discovered that ASC oligomerization detected by chemical cross-linking, and ASC speck formation detected by immunocytochemistry, represent different states of ASC assembly driven by NLRP3. In response to low osmolarity or extracellular ATP stimulation, ASC formed specks as detected by immunofluorescence independently of NLRP3 without activation of caspase-1. These specks were not observed when NLRP3-deficient cells were activated by nigericin, uric acid crystals or *E. coli*. However, ASC oligomerization in response to hypotonicity or ATP (as detected by protein cross-linking and caspase-1 activation) required NLRP3 that localized inside the speck. Our data also revealed that ASC speck formation was controlled through TRP Vanilloid 2 (TRPV2) and TGF-β activated kinase 1 (TAK1) following a decrease in extracellular osmolarity.

MATERIALS AND METHODS

Cells and Reagents

Key reagents and their sources: *E. coli* LPS O55:B5, ATP and nigericin (Sigma); human recombinant IFNγ (PeproTech); 5Z-7-oxozeaenol (Tocris); Uric acid crystals (Invivogen); caspase-1 inhibitor Ac-YVAD-AOM and fluorogenic caspase-1 substrate z-YVAD-AFC (Merck-Millipore); mouse monoclonal anti-V5 and DAPI (Invitrogen); Phalloidin-Texas red (Invitrogen). Abs for ELISAs were from R&D, caspase-1 p10 rabbit polyclonal, IL-1β and ASC from Santa Cruz Biotechnology; mouse monoclonal anti-NLRP3 and mouse monoclonal anti-Caspase-1 p20 from AdipoGen; anti-GFP from Calbiochem; mouse monoclonal anti-flag from Sigma. All HRP-conjugated secondary Abs were from DAKO Cytomation and fluorescent-conjugated secondary Abs from Jackson Immunoresearch.

All animal experiments were carried out under the Animals (Scientific Procedures) Act 1986. Peritoneal and bone marrow macrophages were obtained from male C57BL/6J or from *Nlrp3*$^{-/-}$ or double *Casp-1-Casp11*$^{-/-}$ mice as previously described (14, 24, 25). THP-1 and HEK293 cells were maintained in RPMI1640 and DMEM:F12 (1:1) media respectively, supplemented with 10% fetal calf serum (FCS), 2 mM glutamax and 1 % pen/strep (Invitrogen). Lipofectamine 2000 reagent (Invitrogen) was used for transfecting HEK293 cells under manufacturer's instructions. Biochemical/immunocytochemistry experiments were performed 48 h after transfection. Differentiation and priming of THP-1 cells were performed by overnight incubation in media supplemented with LPS and IFN-γ (100 ng/ml each) and mouse macrophages were primed with LPS (1 μg/ml) for 4 h. Cells were stimulated for different times with an isotonic solution (300 mOsm)

consisting of (in mM) NaCl 147, HEPES 10, glucose 13, $CaCl_2$ 2, $MgCl_2$ 1 and KCl 2; hypotonic solution (90 mOsm) was achieved by diluting the solution 1:4 with distilled sterile water. For TRPV2 gene silencing, THP-1 cells were infected with recombinant lentivirus vectors expressing GFP, random non-targeting shRNA or TRPV2 shRNA; experiments were performed seven days after infection with GFP-positive sorted cells (15).

Immunocytochemistry and microscopy

Macrophages stimulated on coverslips were washed twice with PBS, fixed with 4% formaldehyde, 4% sucrose in PBS for 5 min at room temperature, and then washed three times with PBS. Cells were blocked with 0.5 % bovine serum albumin and permeabilized with 0.1 % triton X-100 in PBS for 5 min at room temperature before incubating with rabbit anti-ASC (1:500), mouse anti-Caspase-1 (1:200) or with mouse anti-NLRP3 (1:1000) for 1 h at 37^{o}C. Cells were washed and incubated with appropriate fluorescence-conjugated secondary antibody (1:200) for 2 h at room temperature, then rinsed in PBS and incubated for 5 min with 300 nM of DAPI. To stain for active caspase-1, macrophages were activated with hypotonic solution for 45 min at 37^{o}C, washed and incubated with the fluorochrome inhibitor of caspase-1, green fluorescent peptide 5-carboxyfluorescein-Tyr-Val-Ala-Asp-fluoromethyl ketone (FAM-YVAD-fmk, FLICA), according to the manufacturer's recommendations (Immunochemistry Technologies). Cells were fixed with 4% formaldehyde, blocked, permeabilized and co-stained for ASC or NLRP3 as described above. All coverslips were mounted on slides with ProLong Gold Antifade Reagent (Invitrogen). Images were acquired either with a Delta Vision RT

(Applied Precision) restoration microscope using a Coolsnap HQ (Photometrics) camera, with a 60x/1.42 Plan Apo or 100x/1.40 Uplan Apo objectives, a Z optical spacing of 0.2 μm and the 360nm/475nm, 490nm/528nm and 555nm/617nm filter sets (Chroma 86000v2); or with a Axiovert 25 microscope (Zeiss) equipped with 40x and 100x objectives and an Axiocam HRc camera (Zeiss). Where mentioned in the text, raw images were then deconvolved using Softworx software and maximum intensity projections of these deconvolved images are shown in the results.

ASC oligomerization

Visualization of ASC oligomerization was performed as previously described (3). Briefly, cells were lysed in buffer A (20 mM HEPES-KOH, pH 7.5, 10 mM KCl, 1.5 mM $MgCl_2$, 1 mM EDTA, 1 mM EGTA, 320 mM sucrose) by passing the lysate 30 times through a 21-gauge needle. The cell lysate was centrifuged and the supernatant was filtered using a 3 μm filter. The supernatant was diluted with one volume of CHAPS buffer (20 mM HEPES-KOH, pH 7.5, 5 mM $MgCl_2$, 0.5 mM EGTA, 0.1 mM PMSF, 0.1 % CHAPS) and then centrifuged to pellet ASC oligomeric complex structures. ASC oligomers were cross-linked using 2 mM NHS-Diazirine (Pierce) for 30 min at 4ºC in CHAPS buffer. After quenching with 20 mM Tris pH 8.8, UV irradiation (using a 365 nm UV bulb) was performed for 10 min at 4°C before adding sample buffer.

Co-immunoprecipitation, western blotting, ELISA, caspase-1 activity and K^+ determination

Detailed methods used for Western blot analysis, caspase-1 activity and ELISAs have been described previously (26, 27). For coIP, equal amounts of protein (500–750 μg) were incubated with 2 μl (1.5 μg) of anti-GFP (Calbiochem) for 1 h at 4ºC on a rotating wheel. After adding prot-G-agarose beads (20 μl per sample) for 1 h at 4ºC, beads were washed three times (5 min at 4ºC) in lysis buffer. Proteins were eluted by heating samples (5 min at 80ºC) in presence of reducing agent and loading sample buffer (Invitrogen). Proteins were separated on 4-12% gradient Bis-tris gels (Invitrogen) and transferred to a nitrocellulose membrane (Millipore). Intracellular K^+ was quantified from THP-1 cell lysates by indirect potenciometry on a Cobas 6000 with ISE module (Roche).

Flow cytometry for extracellular ASC speck determination

For the detection of extracellular particles of ASC, 0.5 ml of cell-free culture supernatants of stimulated macrophages were incubated for 1 h with 1 μg rabbit polyclonal anti-ASC (AdipoGen). Particles were centrifuged and washed before incubation with the secondary antibody Alexa Fluor 647-conjugated goat anti-rabbit IgG (Life Technologies). Samples were washed before being analyzed by flow cytometry with a FACSCanto (BD Biosciences) and FACSDiva software (BD Biosciences) by gating for small particles or cell debris based on forward scatter versus side scatter, adjusted to display correct separation of leukocyte populations. Gated events are presented on plots showing percent of positive particles relative to all small gated particles.

BRET measurements

Transfected HEK293 cells were plated in poly-L-Lysine coated 96 well plate, after adhesion, cells were washed with PBS-CM and readings were then immediately performed after addition of 5 µM coelenterazine-H substrate (Invitrogen) in isotonic or hypotonic solution. Readings were also performed during incubation in a buffer containing 120 mM glycerol with 140 mM NaCl or 140 mM KCl, or following stimulation of the cells with nigericin. Signals were detected with two filter settings (R-Luc filter, 485 ± 20 nm; and YFP filter, 530 ± 25 nm) at 37ºC using the Mithras LB940 plate reader (Berthold Biotechnologies). The BRET ratio was defined as the difference of the emission at 530 nm/485 nm of co-transfected R-Luc and YFP fusion proteins and the emission at 530 nm/485 nm of the R-Luc fusion protein alone. Results were expressed in milliBRET units (mBU). For saturation curves, a constant amount of R-Luc tagged proteins were transfected with increasing quantities of YFP-tagged proteins. The amount of YFP- and R-Luc-tagged proteins was determined by reading on separate plates at 530 nm after excitation at 485 nm and reading at 485 nm in the presence of coelenterazine-H respectively. BRET signals were determined as described above. The BRET experiments have been performed using the ARPEGE Pharmacology Screening-Interactome platform facility at the Institute of Functional Genomic (IGF, Montpellier, France).

Quantitative RT-PCR Analysis (qRT-PCR)

Detailed methods used for qRT-PCR have been described previously (28). Specific primers were purchased from Qiagen (QuantiTech Primer Assays), for each primer set the efficiency was > 95% and a single product was seen on melt curve analysis. Relative

expression levels were calculated using the $2^{-\Delta\Delta Ct}$ method normalizing to GAPDH expression levels for each treatment and the fold increase in expression was relative to the smallest expression level.

LDH release measurements

The presence of LDH in the medium was measured using the Cytotoxicity Detection kit (Roche) following the manufacturer's instructions and expressed as the percent of total amount of LDH in the cells.

Statistical analysis

Data are presented as the mean ± standard error of the mean from the number of assays indicated (from at least three separate experiments). Data were analyzed by an unpaired two-tailed Student's t-test to determine difference between two groups or using a one-way ANOVA with Bonferroni's multiple-comparison test to determine difference between more than two groups using Prism (GraphPad) software.

RESULTS

ASC oligomerizes in response to cell swelling

We have recently described that hypotonicity activates the NLRP3 inflammasome (15). The aim of this study was to investigate the involvement of ASC in this process. Biochemical cross-linking revealed that hypotonic solution induced the oligomerization of ASC, mainly into dimers, but also into higher order complexes (Fig. 1A). As expected, the NLRP3 activator nigericin also induced oligomerization of ASC (Fig. 1A). ASC oligomerization is known to result in pyroptosis, a specific type of cell death driven by ASC-dependent activation of caspase-1 (3, 10). Kinetics of lactate dehydrogenase (LDH) release into macrophage supernatants after 1h exposure to hypotonic solution revealed that the release of LDH was negligible compared to unstimulated macrophages (Fig. 1B). However, LDH release increased up to 20% after 3 h in hypotonic solution (Fig. 1B). In parallel, we measured the release of IL-1β as an indicator of caspase-1 activation, since inhibition of caspase-1 abrogated release of IL-1β (Fig. 1B). After 20 min in hypotonic solution, approximately 40% of the releasable IL-1β was detected in the supernatants of macrophages. The maximum release of IL-1β under these conditions was achieved after 40 min of stimulation with hypotonic solution (Fig. 1B). Pyroptosis is also characterized by cell swelling (3, 10) and we found that macrophage cell swelling induced by hypotonicity was followed by a regulatory volume decrease (RVD), when cells recovered to their initial size (Fig. S1A). We have recently reported that RVD is an essential process for NLRP3 inflammasome activation (15). Absence of ASC, or irreversible inhibition of caspase-1, did not influence cell swelling or RVD kinetics of macrophages

(Fig. S1A). These results suggest that ASC oligomerization and IL-1β release are not coupled with cell death routines at early time points of stimulation by hypotonic solution.

To study macrophage viability at longer times after ASC speck formation, macrophages were incubated for 1h in isotonic or hypotonic solution and then exposed to a normal isotonic cell culture media (Fig. S1B). After 16 h, macrophages pretreated with hypotonic solution demonstrated no apparent cell death as measured by the level of LDH in the supernatant (Fig. 1C), although they still contained ASC oligomers (Fig. 1D). Pro-inflammatory gene expression for IL-1β, IL-12p40, IL-6 and cyclooxygenase-2 induced by lipopolysaccharide (LPS) were also similar between hypotonic or isotonic pretreated macrophages (Fig. 1E), suggesting that LPS priming was not affected by the formation of ASC specks.

ASC oligomerization required TRPV2 signaling and NLRP3

We then studied the effect of cell swelling and RVD modulators on ASC oligomerization. K^+ efflux during cell swelling is important for RVD and for IL-1β processing and release (Fig. S2A-C). This is in agreement with previous work, where intracellular K^+ depletion is an important step for NLRP3 inflammasome activation (15, 29). Prevention of K^+-efflux and RVD by using a glycerol-KCl solution, resulted in a reduction of ASC oligomerization (Fig. 2A). The importance of RVD for ASC oligomerization was also confirmed by using 5-Nitro-2-(3-phenylpropylamino)benzoic acid (NPPB), a blocker of swelling activated Cl^--channel, which impaired RVD (Fig. S2D), caspase-1 activation and ASC oligomerization (Fig. 2B). Similarly, glyburide, a

NLRP3 inhibitor (30), was able to prevent RVD (Fig. S2D) and ASC oligomerization (Fig. 2B).

The activation of the NLRP3 inflammasome during hypotonic stimulation involved TRP channel signaling, while TRPM7 controls RVD, TRPV2 is activated during RVD (15). ASC oligomerization induced by hypotonic solutions was abolished by the broad-spectrum TRP channel inhibitors La^{3+} and 2-Aminoethoxydiphenyl borate (Fig. 2B). Furthermore, effective TRPV2 gene silencing in THP1 macrophages (Fig. S3A,B) resulted in a reduction of both ASC oligomerization and IL-1β release caused by hypotonic solution (Fig. 2C). THP1 infection with control lentivirus carrying a scramble shRNA sequence did not impair ASC oligomerization and IL-1β release induced by hypotonicity (Fig. S3C). High concentrations of Mg^{2+} inhibit TRPM7 (31), consistent with our discovery that decreasing the Mg^{2+} concentration enhanced ASC oligomerization (Fig. 2D).

During the RVD in macrophages, TRP channels modulate an intracellular Ca^{2+} rise that activates TAK1 kinase, which ultimately signals to the NLRP3 inflammasome (15). When intracellular Ca^{2+} was chelated by BAPTA-AM, or when TAK1 activation was inhibited, hypotonic stimulation failed to induce ASC oligomerization and maturation of IL-1β (Fig. 2E). NLRP3 was found to be necessary for ASC oligomerization, since ASC appears monomeric in macrophages deficient in NLRP3 that were exposed to hypotonic solution (Fig. 2F). Altogether, these results suggest that ASC oligomerization could be an important step of signaling for NLRP3 inflammasome formation, and also that the presence of NLRP3 is ultimately required for ASC oligomerization.

ASC forms specks during hypotonic stimulation

Under resting conditions, endogenous ASC was homogeneously distributed throughout the cytosol of macrophages (Fig. 3A and S3D). After 40 min in a hypotonic solution, ASC completely relocated and formed specks (Fig. 3A and S3D). ASC specks were present in 23.2 ± 3.3% of THP-1 cells, and in 27.8 ± 4.2% of mouse primary BMDMs exposed to hypotonic solution. Almost all (87.5 ± 7.9%) of THP-1 cells containing ASC specks also contained active caspase-1 (Fig. 3B). These results suggest that ASC specks are important for the activation of caspase-1 following stimulation with hypotonic solution.

TRPV2 translocates to the plasma membrane during RVD and induces cell permeabilization (15). Macrophage plasma membrane permeabilization was associated with ASC speck formation, since we found 79.6 ± 2.5% of cells with ASC specks positive for Lucifer yellow (Fig. 4A). Consistently, TRPV2 gene silencing in THP1 cells resulted in a reduction of ASC speck formation induced by hypotonicity (Fig. 4B). Finally, ASC specks caused by hypotonic stimulation were also reduced when either intracellular Ca^{2+} was chelated by BAPTA-AM or when TAK1 was inhibited by 5Z-7-oxozeaenol (Fig. 4C). Unexpectedly, NLRP3 deficiency did not affect ASC speck formation after hypotonic stimulation (Fig. 4D), suggesting that NLRP3 is key for ASC oligomerization and caspase-1 activation, but not for ASC speck formation.

We next investigated if other NLRP3 activators could induce ASC speck formation in the absence of NLRP3. As expected, in macrophages from wild-type mice, stimulation with extracellular ATP, nigericin, uric acid crystals or *E. coli*, caused oligomerization of ASC as detected by the appearance of higher molecular weight

complexes of ASC after chemical cross-linking (Fig. 5A). Similar to hypotonicity, all these NLRP3 activators failed to induce ASC oligomerization and IL-1β maturation in the absence of NLRP3 (Fig. 5A). However, NLRP3 deficiency did not affect ASC speck formation after ATP stimulation, but completely prevented it after nigericin, uric acid crystals or *E. coli* challenge (Fig. 5B,C). These data suggest that NLRP3 activation in response to different stimuli could depend upon different dynamics of ASC oligomerization.

A kinetic analysis of ASC oligomerization induced by hypotonicity in wild-type macrophages showed that ASC cross-linking, IL-1β release and caspase-1 activation occurred after 10 min stimulation (Fig. 6A-C). However, whereas strong ASC oligomerization was detected at early time points of stimulation, IL-1β release and caspase-1 activation were almost negligible after 10 min of stimulation. As expected, deficiency of NLRP3 resulted in the absence of ASC cross-linking, IL-1β release or caspase-1 activation at any time point examined after hypotonic stimulation (Fig. 6A-C). ASC specks were found inside both wild-type and NLRP3-deficient macrophages after 10 min of hypotonic stimulation (Fig. 6D). The percentage of cells with ASC specks decreased over the time of stimulation, with this decrease occurring significantly faster in wild-type macrophages when compared to *Nlrp3*$^{-/-}$ macrophages (Fig. 6D). Recent reports show that ASC specks are released from macrophages after formation (27, 32), and we found extracellular ASC specks after hypotonic stimulation in both wild-type and NLRP3-deficient macrophages (Fig. 6E). We observed that the majority of cells containing ASC specks at early time points after stimulation presented more than one speck per cell (Fig. 6F). When multiple ASC specks were present in a cell, they had a

smaller size compared with specks formed at later time points after stimulation (Fig. 6F). When compared to wild-type macrophages, NLRP3-deficient macrophages presented more cells containing multiple ASC specks at late time points of stimulation (Fig. 6F). These data suggest that the large end-point speck found in the majority of wild-type macrophages is an aggregate of smaller ASC specks formed quickly after stimulation. The formation of this big speck appears dependent on NLRP3 and could be the caspase-1-activating platform.

Characterization of ASC and NLRP3 protein dynamics inside the ASC speck

To further study the interaction and dynamics of ASC and NLRP3 complex assembly inside the speck during hypotonic stimulation, we labeled the C-terminus (Ct) of ASC with YFP and the Ct of NLRP3 with *Renilla*-luciferase (Luc) to record bioluminescence resonance energy transfer (BRET, Fig. 7A). Prior to stimulation, ASC-YFP and NLRP3-Luc proteins expressed in HEK293 cells are in spatial proximity to each other, as indicated by a high specific saturated BRET signal (Fig. 7B), and they also co-localized in the cytosol of the cell (Fig. 7C). The non-interacting protein β-arrestin-YFP gave a non-specific linear increase of the BRET signal with NLRP3-Luc (Fig. 7B). Similarly, non-specific BRET due to random collision was found when ASC-YFP was co-expressed with NLRP3-Luc construct truncated at the PYD domain (NLRP3-ΔPYD, Fig. 7B). NLRP3-ΔPYD was also unable to co-localize within the ASC speck (Fig. 7D). These results indicate that the BRET signal between ASC-YFP and NLRP3-Luc was due to a specific interaction of ASC and NLRP3 through the PYD domain.

However, physical interaction between ASC and NLRP3 was not evident by co-immunoprecipitation (coIP) experiments in resting conditions (Fig. 7E,F). After hypotonic cell stimulation, ASC and NLRP3 did coIP (Fig. 7E,F) through specific PYD domain interaction (Fig. 7E,F). This strong interaction after hypotonic stimulation was also evidenced by a fast reduction of the magnitude of the net BRET signal of about 30% (Fig. 7G), suggesting that NLRP3 Leucine-rich repeat and the ASC CARD domains separate from each other during inflammasome activation. Such a conformational change was not observed when K^+ efflux and RVD was prevented by a glycerol-KCl solution (Fig. 7H). Similarly, NLRP3 activation by nigericin also resulted in a fast reduction of the magnitude of the net BRET signal between ASC-YFP and NLRP3-Luc (Fig. 7I). However, while hypotonicity lead to a constantly reduced BRET signal during the recording time the reduction of the BRET signal induced by nigericin quickly recovered (Fig. 7I). These data support the idea that the dynamics of ASC and NLRP3 complex assembly are different during hypotonic or nigericin stimulation. Nigericin induced conformational changes among ASC and NLRP3 were abolished when nigericin was applied in an extracellular buffer containing high K^+ (Fig. 7J). As a control, stimulation of cells expressing a YFP-Luc fusion protein resulted in no variation of net BRET signal (Fig. 7K).

ASC speck formation is associated with the initial activation of the NLRP3 inflammasome

To further elucidate the role of ASC specks during NLRP3 inflammasome activation, we studied the subcellular localization of endogenous ASC, NLRP3 and active

caspase-1 by immunofluorescence in THP-1 macrophages. Under resting conditions, ASC and NLRP3 were homogenously distributed throughout the cytoplasm of macrophages and no FLICA staining was detected (Fig. 8A). Active caspase-1 was detected 20 min after a decrease in extracellular osmolarity, and localized with NLRP3 close to the ASC speck (Fig. 8A). As FLICA impairs caspase-1 auto-cleavage, the localization of caspase-1 we observed could represent an accumulation of inhibited caspase-1 that could not be released from the polymerizing ASC speck. After 40 min in hypotonic solution the NLRP3 and FLICA signals were found throughout the cytoplasm (Fig. 8A). We also found that after hypotonicity, caspase-1 was located in the ASC speck in wild-type, but not in *Nlrp3*$^{-/-}$ or *Casp1-Casp11*$^{-/-}$ macrophages (Fig. 8B), suggesting that NLRP3 was important for recruiting and activating caspase-1 into the ASC oligomer. Consistent with these observations, we found NLRP3 in the purified ASC oligomeric fraction after hypotonic stimulation (Fig. 8C). Similar to murine BMDMs, kinetic analysis during THP-1 macrophage swelling revealed that ASC oligomerization occurred 15 min after the hypotonic challenge (Fig. 8D), which was before active caspase-1 or mature IL-1β could be detected in the cell supernatants (Fig. 8D). Caspase-1 and mature IL-1β release were detected after 25 min of hypotonic stimulation, i.e. at a time where ASC oligomerization was already maximal (Fig. 8D).

Altogether our data suggest that hypotonic extracellular media induced the formation of ASC specks that oligomerized independently of NLRP3, but did not activate caspase-1. Interaction of these ASC specks with NLRP3 PYD domain is therefore necessary to activate caspase-1 in response to hypotonic stimulation.

DISCUSSION

In this study, we found that hypotonic solutions, acting as a danger signal in macrophages, induced a re-localization of ASC into specks which were associated with NLRP3 inflammasome assembly and caspase-1 activation. NLRP3 was not necessary for ASC speck formation in response to hypotonicity or extracellular ATP, however was required for caspase-1 recruitment to the ASC speck and its activation. These results show that certain types of ASC speck were not detected by chemical cross-linking, and that ASC specks formed in the absence of NLRP3 were generally smaller in size. Conventionally, ASC specks detected by immunocytochemistry are considered to represent the same event as ASC oligomers detected by chemical cross-linking (3), with ASC being recognized as an adaptor protein for the NLRP3 inflammasome (2) required for cell-swelling induced caspase-1 activation (15). Here we found that hypotonic stimulation induced ASC speck formation independently of NLRP3 without oligomerization of ASC as detected by chemical cross-linking. In the absence of assembly with NLRP3, these ASC specks failed to activate caspase-1 or IL-1β release.

The ASC speck is the initial structure for pyroptosis, a specific type of cell death driven by caspase-1. ASC specks and pyroptosis are often triggered by infection with intracellular pathogens, or exposure to non-infectious agents like PAMPs or DAMPs (imiquimod, monosodium urate crystals, ATP, α-toxin or lipopeptides) (3, 10, 14). One of the consequences of caspase-1 activation is cell swelling, which could end with pyroptosis (3). Our data demonstrate that ASC speck formation and caspase-1 activation is a result, rather than a cause, of cell swelling followed by a RVD process induced by hypotonic solutions. As such, deficiency for ASC, or caspase-1 inhibition, did not alter

cell swelling and RVD in response to low extracellular osmolarities. Although hypotonic stimulation induced ASC specks, ASC oligomerization, and activation of caspase-1, we found that macrophages remain viable in hypotonic solutions; the ASC specks being a platform for caspase-1 activation independently of cell death. In fact, ASC induced cell death was recently found to be independent of caspase-1 catalytic activity (33), but rather due to a change in the expression of proteins involved in pyroptotic cell death by microbe-infected macrophages. Our study also revealed that ASC oligomerization in response to hypotonic stimulation was irreversible, and in these conditions macrophages maintained their viability and functionality.

Macrophages infected with *Salmonella* activate both NLRP3 and NLRC4 via their recruitment into ASC specks (9, 11), and this mechanism has been proposed as an alternative pathway for inflammasome activation. However, it is unknown whether ASC specks also form a molecular platform for DAMP activation of NLRP3. When expressing ASC and NLRP3 in HEK293 cells, we found ASC in close proximity to NLRP3 during resting conditions, and upon hypotonic stimulation there was a decrease in net BRET signal between both proteins, suggesting that ASC-CARD and NLRP3-LRR domains separate from each other. However, as BRET experiments have been performed in HEK293 cells, we cannot rule out that this interaction could be partially caused by the overexpression of the two proteins. We have previously proposed that this molecular interplay most likely occurs by a compacting or hiding the NLRP3-PYD domain inside the inflammasome complex (15), and here we found that, as expected, the NLRP3-PYD domain is crucial for its interaction with the ASC speck. This protein compaction could explain the lack of NLRP3 staining in the ASC speck (by immunocytochemistry) after

hypotonic stimulation, whereas, NLRP3 localization in the ASC speck was strongly suggested by the coIP experiments. This dual activity of ASC, its self-association into specks and its interaction with NLRP3, was recently suggested when the structure of the PYD domain of ASC was found to contain two different binding sites, one important for self-association and other for NLRP3 interaction (34). The decrease of net BRET signal could also reflect a potential dissociation of ASC and NLRP3 during hypotonic stimulation, although physical interaction between them was observed by coIP after stimulation, suggesting that close proximity of NLRP3 in the ASC speck complexes present a relaxed conformation. In resting conditions, maintaining inflammasome proteins in close proximity does not determine its activation. Thus, we were able to find NLRP3 and ASC colocalization and positive BRET signal, but were not able to identify an association by coIP.

Our data show that cell activation by decreasing extracellular osmolarity or by extracellular ATP induced a rapid assembly of ASC into specks, independent of functional NLRP3, because it occurred in *Nlrp3*$^{-/-}$ macrophages and by co-expression of ASC with NLRP3-ΔPYD, which was unable to localize into the ASC speck. Other NLRP3 activators, such as nigericin, MSU crystals or *E. coli* infection, were unable to induce ASC specks in the absence of NLRP3. These data suggest different dynamics of ASC and NLRP3 complex assembly during activation. Such differences were also suggested by the BRET experiments where differences were observed when cells were activated by hypotonicity or nigericin.

Initial small ASC specks formed in response to hypotonicity are independent of NLRP3. However, aggregation over the time of these specks in a single spot and

oligomerization of ASC as revealed by cross-linking require the presence of NLRP3, which is crucial for caspase-1 activation. Later conformational changes of the ASC speck could serve as a mechanism to spread active caspase-1 through the cytosol, as has already been described for pyroptosis (10). Current models for NLRP3 inflammasome activation suggest that upon macrophage stimulation by danger signals, NLRP3 oligomerize and then recruit ASC in fiber-like structures that amplify caspase-1 activation (5, 6). Our results also suggest that NLRP3 is necessary to form a compact ASC structure, probably through the tight oligomerization of ASC. A recent study has also shown that in response to *Salmonella*, NLRP3 and NLRC4 localize to the same ASC speck (11) suggesting a central role for ASC speck in inflammasome formation and/or activation. Our results show that after hypotonicity or ATP stimulation, small ASC specks appear in wild-type and *Nlrp3*$^{-/-}$ macrophages and that the presence of NLRP3 is important for developing ASC specks to form large irregular structures that recruit and activate caspase-1. In the absence of NLRP3, ASC specks fail to recruit and activate caspase-1. Although ASC can self-aggregate and activate caspase-1 when macrophages are infected with different bacteria or when overexpressed in HEK293 cells (27), we cannot rule out that, in macrophages deficient in NLRP3, inactive ASC specks formed in response to hypotonicity could be induced by another receptor. However, our data could also suggest an alternative model for inflammasome assembly in response to hypotonicity or ATP stimulation, where the small inactive ASC specks may represent aggregates that will then assemble with NLRP3 to form an inflammasome. Following NLRP3 activation, NLRP3 would interact with these small ASC specks and induce ASC oligomerization detected by cross-linking, leading to the formation of a single ASC speck where caspase-1 would be

activated. Thought this model does not seem to be extendable to all NLRP3 activators, as our experiments point out that nigericin, MSU crystals or *E. coli* activation do not induce ASC specks formation in the absence of NLRP3. Therefore, we cannot exclude that formation of small ASC specks and NLRP3 inflammasome assembly with ASC might represent two different processes where ASC specks observed in the absence of NLRP3 might be involved in inflammasome independent function. In fact, it is known that ASC modulates immune cell functions via expression of Dock2 and Rac activation independently of NLRP3 inflammasome and caspase-1 (35). Moreover, currently available methods do not allow direct measurement of NLRP3 activation but only allow the downstream consequences of inflammasome activation to be measured; therefore we have set up a BRET technique to fill this gap and measure NLRP3 oligomerization and association with ASC in real time (ref. (15) and present work). However, by using different techniques it is difficult to define which of the events occur first during inflammasome activation: single ASC speck formation imagined by immunofluorescence or ASC oligomerization assessed by cross-linking and caspase-1 activation. Finally, we were unable to find IL-1β in the ASC speck, which is consistent with our recent findings where using a specific biosensor to measure pro-IL-1β processing in real time and *in situ*, we showed that cytokine cleavage occurs throughout the cytosol (36). These observations suggest that ASC specks do not represent the main subcellular compartment where the cytokine is processed to its mature form.

We also found here that the signaling pathways that activate the NLRP3 inflammasome in response to hypotonicity (15, 37) are the same as for ASC oligomerization as detected by chemical cross-linking. Both were dependent on low

intracellular potassium concentration, the RVD, TRPM7 and TRPV2 activation, intracellular Ca^{2+} increase and activation of TAK1 kinase. This is not surprising since in the current inflammasome assembly model, NLRP3 is obligatory to induce ASC oligomerization, so everything affecting the activation of NLRP3 is likely to affect downstream ASC oligomer formation. However, our data also show similar striking resemblances for the NLRP3-independent formation of ASC specks, which were dependent on TRPV2 channel activation during cellular RVD and TAK1 phosphorylation. These data indicate that TAK1 might regulate NLRP3 inflammasome activation through the control of ASC speck formation and suggest that both events, ASC speck formation and NLRP3 inflammasome activation, share the same intracellular signaling pathway. In fact potassium efflux appears as a common denominator not only for NLRP3 activation (2, 29, 38, 39), but also for ASC speck formation (3). This observation could explain why other inflammasomes besides NLRP3 also seem to require low intracellular potassium concentration to be functional under certain conditions (40). In a recent publication it was argued that hypotonic stimulation of macrophages was inducing NLRP3 activation through the low K^+ concentration of the extracellular hypotonic buffer used and not via cell swelling and RVD (29). However, our previous work demonstrates that increasing osmolarity of the hypotonic solution with mannitol or sorbitol, and keeping the same low K^+ concentration of the extracellular buffer, abolished the activation of NLRP3, as well as the induction of cell swelling and RVD (15). Also, inhibitors of Cl^- and TRP channels abolished RVD and NLRP3-dpendent caspase-1 activation, but did not affect intracellular K^+ depletion (15). Furthermore, a recent report found that macrophages deficient in aquaporin 1, or by blocking aquaporin function,

resulted in impaired caspase-1 and IL-1β release in response to hypotonicity induced cell swelling (41). All these data suggest that K^+ efflux from macrophages *per se* is required, but not sufficient to induce inflammasome activation.

Another striking similarity, which we found between ASC oligomerization and NLRP3 inflammasome activation, was their sensitivity to the blocker glyburide. Glyburide is known to selectively block NLRP3 inflammasome formation by acting in an undefined way upstream of NLRP3 (30), and here we found that glyburide also affected ASC oligomerization after hypotonic stimulation by affecting the RVD process. This effect is also similar to the inhibition of the NLRP3 inflammasome by CRID3, which targets ASC oligomerization (18). Recently, it has been found that ASC specks are released from macrophages after inflammasome stimulation and act extracellularly as a danger signal to propagate inflammation (27, 32). Here we found that in contrast with IL-1β release, hypotonicity induced release of ASC specks in the absence of NLRP3, suggesting that the release of ASC specks could be a potent inflammatory mediator broader than IL-1β cytokine release. Consistent with this, blockage of extracellular ASC specks has been found to reduce traumatic brain injury (42). Thus, ASC is emerging as a potential target for which highly selective drugs would block the inflammasome and IL-1β signaling.

Altogether, our data demonstrate that during macrophage swelling, ASC speck formation and oligomerization share the same signaling pathway as NLRP3 inflammasome activation, which includes TRPV2 activation, intracellular Ca^{2+} increase and TAK1 signaling. However, speck formation identified by immunocytochemistry occurred independently of NLRP3, and did not lead to caspase-1 activation. Meanwhile

ASC oligomers detected by immunocytochemistry and chemical cross-linking were only formed in the presence of NLRP3, and leads to functional inflammasomes and activate caspase-1 in response to hypotonic stimulation.

Acknowledgements

We thank V. Dixit for *Nlrp3*$^{-/-}$ mice, E. Latz for ASC deficient mouse bone marrow immortalized macrophages, and J. Tschopp for NLRP3-flag, G. Dubyak for ASC-V5 and J.P. Pin for β-arrestin-YFP expression vectors. We thank E. Martin, R. Gaskell and M.C. Baños for both molecular and cellular technical assistance.

Author contributions

V.C. contributed to design, execution and analysis of experiments of Figures 1A,D, 2, 3, 4, 7B-F,G,I and 8A,C,D. F.M-S. A.B-M., G.L-C. and A.I.G. performed, analyzed and interpreted *in vitro* experiments of Figures 1B,C,E, 5, 6, 7H,J,K and 8B. D.B. provided NLRP3 deficient mice. V.C., D.B. and A.V. contribute to the writing of the manuscript. P.P. conceived, designed and supervised this study, analyzed and interpreted experiments and wrote the final manuscript.

Disclosures

The authors declare no competing financial interests.

REFERENCES

1. Takeuchi, O., and S. Akira. 2010. Pattern recognition receptors and inflammation. *Cell* 140: 805-820.
2. Schroder, K., and J. Tschopp. 2010. The inflammasomes. *Cell* 140: 821-832.
3. Fernandes-Alnemri, T., J. Wu, J.-W. Yu, P. Datta, B. Miller, W. Jankowski, S. Rosenberg, J. Zhang, and E. S. Alnemri. 2007. The pyroptosome: a supramolecular assembly of ASC dimers mediating inflammatory cell death via caspase-1 activation. *Cell Death Differ* 14: 1590-1604.
4. Miao, E. A., I. A. Leaf, P. M. Treuting, D. P. Mao, M. Dors, A. Sarkar, S. E. Warren, M. D. Wewers, and A. Aderem. 2010. Caspase-1-induced pyroptosis is an innate immune effector mechanism against intracellular bacteria. *Nat Immunol* 11: 1136-1142.
5. Cai, X., J. Chen, H. Xu, S. Liu, Q. X. Jiang, R. Halfmann, and Z. J. Chen. 2014. Prion-like Polymerization Underlies Signal Transduction in Antiviral Immune Defense and Inflammasome Activation. *Cell* 156: 1207-1222.
6. Lu, A., V. G. Magupalli, J. Ruan, Q. Yin, M. K. Atianand, M. R. Vos, G. F. Schroder, K. A. Fitzgerald, H. Wu, and E. H. Egelman. 2014. Unified Polymerization Mechanism for the Assembly of ASC-Dependent Inflammasomes. *Cell* 156: 1193-1206.
7. Mariathasan, S., K. Newton, D. M. Monack, D. Vucic, D. M. French, W. P. Lee, M. Roose-Girma, S. Erickson, and V. M. Dixit. 2004. Differential activation of the inflammasome by caspase-1 adaptors ASC and Ipaf. *Nature* 430: 213-218.
8. Martinon, F., K. Burns, and J. Tschopp. 2002. The inflammasome: a molecular platform triggering activation of inflammatory caspases and processing of proIL-beta. *Molecular Cell* 10: 417-426.
9. Broz, P., K. Newton, M. Lamkanfi, S. Mariathasan, V. M. Dixit, and D. M. Monack. 2010. Redundant roles for inflammasome receptors NLRP3 and NLRC4 in host defense against Salmonella. *J Exp Med* 207: 1745-1755.

10. Miao, E. A., J. V. Rajan, and A. Aderem. 2011. Caspase-1-induced pyroptotic cell death. *Immunol Rev* 243: 206-214.
11. Man, S. M., L. J. Hopkins, E. Nugent, S. Cox, I. M. Gluck, P. Tourlomousis, J. A. Wright, P. Cicuta, T. P. Monie, and C. E. Bryant. 2014. Inflammasome activation causes dual recruitment of NLRC4 and NLRP3 to the same macromolecular complex. *Proc Natl Acad Sci U S A* 111: 7403-7408.
12. Martinon, F., V. Pétrilli, A. Mayor, A. Tardivel, and J. Tschopp. 2006. Gout-associated uric acid crystals activate the NALP3 inflammasome. *Nature* 440: 237-241.
13. Duewell, P., H. Kono, K. J. Rayner, C. M. Sirois, G. Vladimer, F. G. Bauernfeind, G. S. Abela, L. Franchi, G. Nuñez, M. Schnurr, T. Espevik, E. Lien, K. A. Fitzgerald, K. L. Rock, K. J. Moore, S. D. Wright, V. Hornung, and E. Latz. 2010. NLRP3 inflammasomes are required for atherogenesis and activated by cholesterol crystals. *Nature* 464: 1357-1361.
14. Mariathasan, S., D. S. Weiss, K. Newton, J. McBride, K. O'Rourke, M. Roose-Girma, W. P. Lee, Y. Weinrauch, D. M. Monack, and V. M. Dixit. 2006. Cryopyrin activates the inflammasome in response to toxins and ATP. *Nature* 440: 228-232.
15. Compan, V., A. Baroja-Mazo, G. López-Castejón, A. Gómez, C. Martínez, D. Angosto, M. T. Montero, A. S. Herranz, E. Bazán, D. Reimers, V. Mulero, and P. Pelegrin. 2012. Cell volume regulation modulates NLRP3 inflammasome activation. *Immunity* 37: 487-500.
16. Stehlik, C., and A. Dorfleutner. 2007. COPs and POPs: modulators of inflammasome activity. *J Immunol* 179: 7993-7998.
17. Laliberte, R. E., D. G. Perregaux, L. R. Hoth, P. J. Rosner, C. K. Jordan, K. M. Peese, J. F. Eggler, M. A. Dombroski, K. F. Geoghegan, and C. A. Gabel. 2003. Glutathione s-transferase omega 1-1 is a target of cytokine release inhibitory drugs and may be responsible for their effect on interleukin-1beta posttranslational processing. *J Biol Chem* 278: 16567-16578.

18. Coll, R. C., and L. A. J. O'Neill. 2011. The Cytokine Release Inhibitory Drug CRID3 Targets ASC Oligomerisation in the NLRP3 and AIM2 Inflammasomes. *PLoS ONE* 6: e29539.

19. Henao-Mejia, J., E. Elinav, C. Jin, L. Hao, W. Z. Mehal, T. Strowig, C. A. Thaiss, A. L. Kau, S. C. Eisenbarth, M. J. Jurczak, J.-P. Camporez, G. I. Shulman, J. I. Gordon, H. M. Hoffman, and R. A. Flavell. 2012. Inflammasome-mediated dysbiosis regulates progression of NAFLD and obesity. *Nature* 482: 179-185.

20. Halle, A., V. Hornung, G. C. Petzold, C. R. Stewart, B. G. Monks, T. Reinheckel, K. A. Fitzgerald, E. Latz, K. J. Moore, and D. T. Golenbock. 2008. The NALP3 inflammasome is involved in the innate immune response to amyloid-beta. *Nat Immunol* 9: 857-865.

21. de Rivero Vaccari, J. P., G. Lotocki, A. E. Marcillo, W. D. Dietrich, and R. W. Keane. 2008. A molecular platform in neurons regulates inflammation after spinal cord injury. *J Neurosci* 28: 3404-3414.

22. Vandanmagsar, B., Y.-H. Youm, A. Ravussin, J. E. Galgani, K. Stadler, R. L. Mynatt, E. Ravussin, J. M. Stephens, and V. D. Dixit. 2011. The NLRP3 inflammasome instigates obesity-induced inflammation and insulin resistance. *Nat Med* 17: 179-188.

23. Riteau, N., P. Gasse, L. Fauconnier, A. Gombault, M. Couegnat, L. Fick, J. Kanellopoulos, V. F. J. Quesniaux, S. Marchand-Adam, B. Crestani, B. Ryffel, and I. Couillin. 2010. Extracellular ATP is a danger signal activating P2X7 receptor in lung inflammation and fibrosis. *Am J Respir Crit Care Med* 182: 774-783.

24. Lopez-Castejon, G., J. Theaker, P. Pelegrin, A. D. Clifton, M. Braddock, and A. Surprenant. 2010. P2X7 Receptor-Mediated Release of Cathepsins from Macrophages Is a Cytokine-Independent Mechanism Potentially Involved in Joint Diseases. *J Immunol* 185: 2611-2619.

25. Kuida, K., J. A. Lippke, G. Ku, M. W. Harding, D. J. Livingston, M. S. Su, and R. A. Flavell. 1995. Altered cytokine export and apoptosis in mice deficient in interleukin-1 beta converting enzyme. *Science* 267: 2000-2003.

26. Pelegrin, P., and A. Surprenant. 2006. Pannexin-1 mediates large pore formation and interleukin-1beta release by the ATP-gated P2X7 receptor. *EMBO J* 25: 5071-5082.

27. Baroja-Mazo, A., F. Martín-Sanchez, A. Gomez, C. M. Martínez, J. Amores-Iniesta, V. Compan, M. Barberà-Cremades, J. Yagüe, E. Ruiz-Ortiz, J. Antón, S. Buján, I. Couillin, D. Brough, J. I. Arostegui, and P. Pelegrin. 2014. The NLRP3 inflammasome is released as a particulate danger signal that amplifies the inflammatory response. *Nat Immunol* doi:10.1038/ni.2919.

28. Pelegrin, P., and A. Surprenant. 2009. Dynamics of macrophage polarization reveal new mechanism to inhibit IL-1beta release through pyrophosphates. *EMBO J* 28: 2114-2127.

29. Munoz-Planillo, R., P. Kuffa, G. Martinez-Colon, B. L. Smith, T. M. Rajendiran, and G. Nunez. 2013. K(+) Efflux Is the Common Trigger of NLRP3 Inflammasome Activation by Bacterial Toxins and Particulate Matter. *Immunity* 38: 1142-1153.

30. Lamkanfi, M., J. L. Mueller, A. C. Vitari, S. Misaghi, A. Fedorova, K. Deshayes, W. P. Lee, H. M. Hoffman, and V. M. Dixit. 2009. Glyburide inhibits the Cryopyrin/Nalp3 inflammasome. *J Cell Biol* 187: 61-70.

31. Penner, R., and A. Fleig. 2007. The Mg2+ and Mg(2+)-nucleotide-regulated channel-kinase TRPM7. *Handb Exp Pharmacol*: 313-328.

32. Franklin, B., L. Bossaller, D. De Nardo, J. MRatter, A. Stutz, G. Engels, C. Brenker, M. Nordhoff, S. Mirandola, A. Al-Amoudi, M. Mangan, S. Zimmer, B. G. Monks, M. Fricke, R. Schmid, T. Espevik, B. Jones, A. Jarnicki, P. Hansbro, P. Busto, A. Marshak-Rothstein, S. Hornemann, A. Aguzzi, W. Kastenmuller, and E. Latz. 2014. The adaptor ASC has extracellular and 'prionoid' activities that propagate inflammation. *Nat Immunol* doi:10.1038/ni.2913.

33. Motani, K., H. Kushiyama, R. Imamura, T. Kinoshita, T. Nishiuchi, and T. Suda. 2011. Caspase-1 protein induces apoptosis-associated speck-like protein containing a caspase recruitment domain (ASC)-mediated necrosis independently of its catalytic activity. *J Biol Chem* 286: 33963-33972.

34. Vajjhala, P. R., R. E. Mirams, and J. M. Hill. 2012. Multiple Binding Sites on the Pyrin Domain of ASC Protein Allow Self-association and Interaction with NLRP3 Protein. *J Biol Chem* 287: 41732-41743.

35. Ippagunta, S. K., R. K. S. Malireddi, P. J. Shaw, G. A. Neale, L. Vande Walle, D. R. Green, Y. Fukui, M. Lamkanfi, and T.-D. Kanneganti. 2011. The inflammasome adaptor ASC regulates the function of adaptive immune cells by controlling Dock2-mediated Rac activation and actin polymerization. *Nat Immunol* 12: 1010-1016.

36. Compan, V., A. Baroja-Mazo, L. Bragg, A. Verkhratsky, J. Perroy, and P. Pelegrin. 2012. A Genetically Encoded IL-1β Bioluminescence Resonance Energy Transfer Sensor To Monitor Inflammasome Activity. *J Immunol* 189: 2131-2137.

37. Gong, Y.-N., X. Wang, J. Wang, Z. Yang, S. Li, J. Yang, L. Liu, X. Lei, and F. Shao. 2010. Chemical probing reveals insights into the signaling mechanism of inflammasome activation. *Cell Res* 20: 1289-1305.

38. Perregaux, D. G., and C. A. Gabel. 1994. Interleukin-1 beta maturation and release in response to ATP and nigericin. Evidence that potassium depletion mediated by these agents is a necessary and common feature of their activity. *J Biol Chem* 269: 15195-15203.

39. Kahlenberg, J. M., and G. R. Dubyak. 2004. Mechanisms of caspase-1 activation by P2X7 receptor-mediated K+ release. *Am J Physiol-Cell Ph* 286: C1100-1108.

40. Lindestam Arlehamn, C. S., V. Pétrilli, O. Gross, J. Tschopp, and T. J. Evans. 2010. The role of potassium in inflammasome activation by bacteria. *J Biol Chem* 285: 10508-10518.

41. Rabolli, V., L. Wallemme, S. Lo Re, F. Uwambayinema, M. Palmai-Pallag, L. Thomassen, D. Tyteca, J. N. Octave, E. Marbaix, D. Lison, O. Devuyst, and F. Huaux. 2014. Critical role of aquaporins in IL-1beta-mediated inflammation. *J Biol Chem*.

42. de Rivero Vaccari, J., G. Lotocki, O. Alonso, H. Bramlett, W. Dietrich, and R. Keane. 2009. Therapeutic neutralization of the NLRP1 inflammasome reduces the

innate immune response and improves histopathology after traumatic brain injury. *J Cereb Blood Flow Metab*.

FOOTNOTES

[§]**Present address**: Institut de Génomique Fonctionnelle, CNRS UMR 5203, INSERM U661, Université de Montpellier 1 & 2, Montpellier, France.

Contact: Dr. Pablo Pelegrín or Dr. Fátima Martín-Sánchez, Inflammation and Experimental Surgery Unit, University Hospital "Virgen Arrixaca", Carretera Madrid Cartagena s/n, 30120 Murcia, Spain. Tel: +34 968 369 317; Fax: +34 968 369 364; e-mail: pablo.pelegrin@ffis.es or fatima.martin@ffis.es

Funding: This work was supported by grants from PN I+D+I 2008-2011-Instituto Salud Carlos III-FEDER (EMER07/049 and PI09/0120), Fundación Séneca (11922/PI/09) and European Research Council (ERC-2013-CoG 614578). V. Compan was supported by grant from Wellcome Trust.

Abbreviations: ASC, apoptosis-associated speck-like protein containing a CARD; BAPTA-AM, 1,2-Bis(2-aminophenoxy)ethane-N,N,N',N'-tetraacetic acid tetrakis-acetoxymethyl ester; BRET, bioluminescence resonance energy transfer; CARD, caspase recruitment domain; coIP, co-immunoprecipitation; DAMP, danger-associated molecular pattern; FLICA, fluorescent labeled inhibitor of caspase-1; IL, interleukin; LDH, lactate dehydrogenase; LPS, lipopolysaccharide; Luc, *Renilla* Luciferase; mOsm, milliosmole; NLR, nucleotide binding and leucine rich repeat receptors; NPPB, 5-Nitro-2-(3-phenylpropylamino)benzoic acid; PAMP, pathogen-associated molecular pattern; PRR,

pattern-recognition receptors; PYD, pyrin domain; RVD, regulatory volume decrease; TAK1, TGF-β activated kinase 1; TRPV, transient receptor potential vanilloid.

FIGURE LEGENDS

Figure 1. Hypotonic stimulation induces ASC oligomerization independently of cell death. (**A**) ASC, caspase-1 and IL-1β Western blot from purified cross-linked ASC oligomer proteins (*ASC Oligomer*), total cell extracts (*Cells*) and cell supernatants (*Sups*) of THP-1 cells primed with LPS and IFN-γ (100 ng/ml each, 16 h) and subsequently stimulated with either a 300 or 90 mOsm extracellular solution for 40 min or with nigericin (25 μM, 30 min). (**B**) Kinetics of IL-1β release measured by ELISA (black trace) and LDH release (grey trace) from THP-1 cells activated as in (A) for different times (left panel), or for 60 min in the presence or absence of a caspase-1 inhibitor (Ac-YVAD, 100 μM). Results represent is the average and s.e.m. of n = 3-6 independent experiments for the different time points. Maximum concentration of released IL-1β used for normalization in left panel was 598.67±93 pg/ml; % of LDH in left panel was normalized to total intracellular LDH content. (**C**) LDH release from primary mouse BMDMs challenged by hypotonic or isotonic solution for 1 h, subsequent culture in isotonic complete cell culture media for 16 h and then primed or not with LPS (1 μg/ml, 4 h); results represent the average and s.e.m. of n = 3 independent experiments. (**D**) ASC Western blot from purified cross-linked ASC oligomer proteins (*ASC Oligomer*) and total cell extracts (*Cells*) in cells treated as indicated in (C). (**E**) Gene expression in cells treated as in (C); represented is the average and s.e.m. of n = 3 independent experiments. Western blots are representative of 4-6 independent experiments.

Figure 2. ASC oligomerization depends upon NLRP3. Western blot from purified cross-linked ASC oligomer proteins (*ASC Oligomer*), total cell extracts (*Cells*) or cell

supernatants (*Sups*) of THP-1 cells primed with LPS and IFNγ (100 ng/ml each, 16 h). (**A**) ASC western blot from cells incubated for different times (0, 20 or 40 min) with two different hypotonic solutions: 120 mM glycerol with 140 mM of NaCl (Na^+ Gly) or 140 mM of KCl (K^+ Gly). (**B**) ASC and caspase-1 western blot from THP-1 activated as in (A) and treated as indicated with La^{3+} (La, 2 mM), 2-Aminoethoxydiphenyl borate (2-APB, 100 μM), NPPB (100 μM) or Glyburide (100 μM). (**C**) ASC and IL-1β western blot from uninfected THP-1 macrophages (control cells), or infected with GFP and non-sense shRNA-lentivirus (Lv-GFP) or lentivirus coding for GFP and TRPV2 shRNA (Lv-shRNA), and subsequently stimulated as in (A). (**D**) ASC western blot from THP-1 activated as in (A) and treated with different concentrations of $MgCl_2$ as indicated. (**E**) ASC, TAK1, Phospho-TAK1 (P-TAK1) and IL-1β Western blot of THP-1 cells primed as in (A) and treated with BAPTA-AM (100 μM) or 5Z-7-oxozeaenol (OXO, 100 μM) as indicated. (**F**) ASC, NLRP3, caspase-1 and IL-1β Western blot of bone marrow derived macrophages from wild type (WT) or NLRP3 deficient (*Nlrp3*$^{-/-}$) mice primed with LPS (1 μg/ml, 4 h) and incubated for 1 h with either an isotonic or hypotonic solution. Western blots are representative of 2 to 4 independent experiments.

Figure 3. ASC speck is associated with caspase-1 activation. (**A**) Representative images of THP-1 macrophages primed with LPS and IFN-γ (100 ng/ml each, 16 h) and subsequently subjected to different extracellular osmolarities for 40 min, stained for ASC (red) and nuclei (DAPI, blue); scale bar 10 μm (upper panel) and 20 μm (lower panel); arrowhead denotes ASC speck. (**B**) Representative images of THP-1 macrophages primed as in (A), stained with fluorescent probe for active caspase-1 (FLICA, green),

ASC (red) and nuclei (DAPI, blue); scale bar 10 μm; arrowhead denotes ASC speck and dashed square denotes cell inset.

Figure 4. TRPV2 channels control ASC speck formation via TAK1 activation in response to hypotonicity. (**A**) Lucifer yellow uptake and ASC speck formation in THP-1 cells primed with LPS and IFN-γ (100 ng/ml each, 16 h) and subsequently subjected to different osmolarities as indicated for 40 min; scale bar 20 μm; arrowheads represent cells with ASC speck and positive for Lucifer yellow; asterisks represent cells with ASC speck and negative for Lucifer yellow. Graphic on the right shows the percentage of cells stimulated with hypotonic solution and presenting either: ASC speck (1), ASC speck but no staining for Lucifer yellow (2), ASC speck and a positive staining for Lucifer yellow (3), a positive staining for Lucifer yellow (4), or a positive staining for Lucifer yellow without ASC speck (5); each dot represents the percentage of $n > 50$ cells. (**B**) Representative images of uninfected control THP-1 macrophages (no-Lv) or infected with GFP-lentivirus (Lv-GFP) or with lentivirus coding for GFP and TRPV2 shRNA (Lv-shRNA), stimulated as in (A), stained for ASC (red, upper panels) and GFP (lower panel, green); arrowheads denote ASC specks; scale bar 40 μm; right histogram shows the average quantification and s.e.m. of cells containing ASC specks from $n = 3$ experiments with $n > 300$ cells per experiment. (**C**) Representative images of THP-1 macrophages stimulated as in (A) and treated with BAPTA-AM (100 μM) or 5Z-7-oxozeaenol (OXO, 100 μM) as indicated; stained for ASC (red) and DAPI (blue); scale bar 40 μm; arrowhead denotes ASC specks; right histogram shows the average quantification and s.e.m. of cells containing ASC specks of $n > 300$ cells from 3

independent experiments. (**D**) High resolution images of mouse peritoneal macrophages from wild type (WT) or NLRP3 deficient (*Nlrp3*$^{-/-}$) mice primed with LPS (1 μg/ml, 4 h) and incubated for 1 h with either an isotonic or hypotonic solution; stained for ASC (red) and DAPI (blue); scale bar 5 μm; right histogram shows the average quantification and s.e.m. of cells containing ASC specks of $n > 300$ cells from 4 independent experiments.

Figure 5. ASC oligomerization is impaired in the absence of NLRP3. (**A**) Western blot from purified cross-linked ASC oligomer proteins (*ASC Oligomer*), total cell extracts (*Cells*) or cell supernatants (*Sups*) of wild-type (WT) or *Nlrp3*$^{-/-}$ BMDMs primed with LPS (1 μg/ml, 4 h), followed by no stimulation (-) or stimulation (+) with ATP (5 mM, 30 min), nigericin (20 μM, 30 min), uric acid crystals (MSU, 200 mg/ml, 16 h) or *E. coli* (MOI 20, 16 h). (**B,C**) Representative images (**B**) and average quantification and s.e.m. (**C**) of cells containing ASC specks from BMDMs primed as in (A); $n = 2$ experiments with $n > 500$ cells per experiment.

Figure 6. Small ASC specks could be formed in the absence of NLRP3 and released from macrophages. (**A**) ASC Western blot of WT or *Nlrp3*$^{-/-}$ mouse BMDMs primed with LPS (1 μg/ml, 4 h) and incubated for 0-60 min with hypotonic solution (90 mOsm). Western blots are representative of 2 independent experiments. (**B-D**) Extracellular IL-1β detection by ELISA (**B**), caspase-1 activity measured by fluorogenic peptide cleavage z-YVAD-AFC (**C**) or percentage of cells containing ASC specks (**D**) after treatment indicated in (A); data represent the average and s.e.m. of $n = 2$ independent experiments (B-D), with $n > 1000$ cells for (D). (**E**) Frequency of extracellular ASC positive particles

detected by flow cytometry in cell-free supernatants of wild-type or *Nlrp3*$^{-/-}$ macrophages primed as in (A) for 60 min, presented as relative value to the total particles gated for small particles; data represent the average and s.e.m. of n = 3 experiments. (**F**) Monochromatic images of BMDMs treated as in (A) for 10 or 45 min and stained for ASC; arrowheads and arrows indicate multiple ASC aggregates or a single ASC aggregate in the cell respectively; scale bar 2 μm. Histogram on the right shows the percentage and s.e.m. of cells containing single or multiple ASC specks relative to the total number of cells containing ASC specks; n > 1000 cells from 2 independent experiments.

Figure 7. NLRP3 interacts with the ASC speck. (**A**) Schematic representation showing NLRP3 BRET donor and ASC acceptor. (**B**) BRET saturation curve for HEK293 cells transfected with a constant quantity of NLRP3-Luc-Ct (continuous lines) or NLRP3-ΔPYD-Luc-Ct (dotted line) and increasing amounts of the BRET acceptor ASC-YFP (black circles and open triangles) or β-arrestin-YFP (open circles). (**C**) Image of HEK293 cells transfected with NLRP3 (red) and ASC-YFP (green). Nuclei stained with DAPI (blue); scale bar 10 μm. (**D**) Quantification of NLRP3 and NLRP3-ΔPYD in the ASC speck, data represent average and s.e.m. of $n \geq 36$ cells from 3 independent experiments. (**E**) NLRP3-flag and ASC-V5-YFP coIP after HEK293 cells incubation for 40 min in isotonic or hypotonic solution. Western blot is representative of 3 independent experiments. (**F**) NLRP3-flag or NLRP3-ΔPYD-flag and ASC-V5 coIP after HEK293 cells incubation for 40 min in hypotonic solution. Western blot is representative of 2 independent experiments. (**G**) Kinetics of net BRET signal in HEK293 cells transfected

with the BRET donor NLRP3-Luc-Ct and the acceptor ASC-YFP in response to isotonic (grey circles) or hypotonic solution (white circles); hypotonicity was induced when indicated by an arrow; representation is average and s.e.m. of 3-4 independent experiments. (**H**) Percentage of net BRET signal reduction of cells transfected as in (G) after 20 min in a solution with 120 mM glycerol and either 140 mM NaCl (Na^+-Gly) or 140 mM KCl (K^+-Gly); representation is average and s.e.m. of 4 independent experiments. (**I**) Kinetics of net BRET signal recorded as in (G) in response to vehicle (grey circles) or nigericin (20 μM, black circles); nigericin was injected when indicated by an arrow; representation is average and s.e.m. of 3 independent experiments. (**J**) Percentage of net BRET signal reduction of cells treated as in (I) after 2 min stimulation with nigericin in normal or high extracellular K^+ concentration; representation is average and s.e.m. of 2 independent experiments. (**K**) Kinetics of net BRET signal in HEK293 cells transfected with a Luc-YFP fusion construct (BRET control protein) in response to isotonicity (white circles), hypotonicity (light grey circles), 120 mM glycerol solution with 140 mM NaCl (Na^+-Gly, dark grey circles) or nigericin (black circles); stimulation was induced when indicated by an arrow; representation is average and s.e.m. of 3 independent experiments.

Figure 8. ASC speck formation is associated with the initial assembly of the NLRP3 inflammasome. (**A**) High-resolution images of THP-1 macrophages primed with LPS and IFN-γ (100 ng/ml each, 16 h) and subsequently subjected to hypotonic extracellular solution for different times as indicated, stained for ASC (blue, middle row of panels), NLRP3 (red, bottom row of panels) and for active caspase-1 using FLICA reagent (green,

upper row of panels); scale bar 10 μm; arrowhead denotes ASC speck localization. (**B**) Images of wild-type, *Nlrp3*$^{-/-}$ or *Casp1-Casp11*$^{-/-}$ BMDMs primed with LPS (1 μg/ml, 4h) and then stimulated with hypotonicity (90 mOsm, 45 min) and stained for ASC (green) and caspase-1 (red); scale bar 10 μm. (**C**) NLRP3 Western blot on purified ASC oligomeric fraction (*ASC Oligomer*) and total cell extracts (*Cells*) in THP-1 cells treated as indicated in (A). Western blot is representative of 2 independent experiments. (**D**) ASC, IL-1β and caspase-1 Western blot of purified cross-linked ASC oligomer proteins (*ASC Oligomer*), total cell extracts (*Cells*) and cell supernatants (*Sups*) in THP-1 cells treated as indicated in (A); RVD: regulatory volume decrease. Western blot is representative of 2 independent experiments.

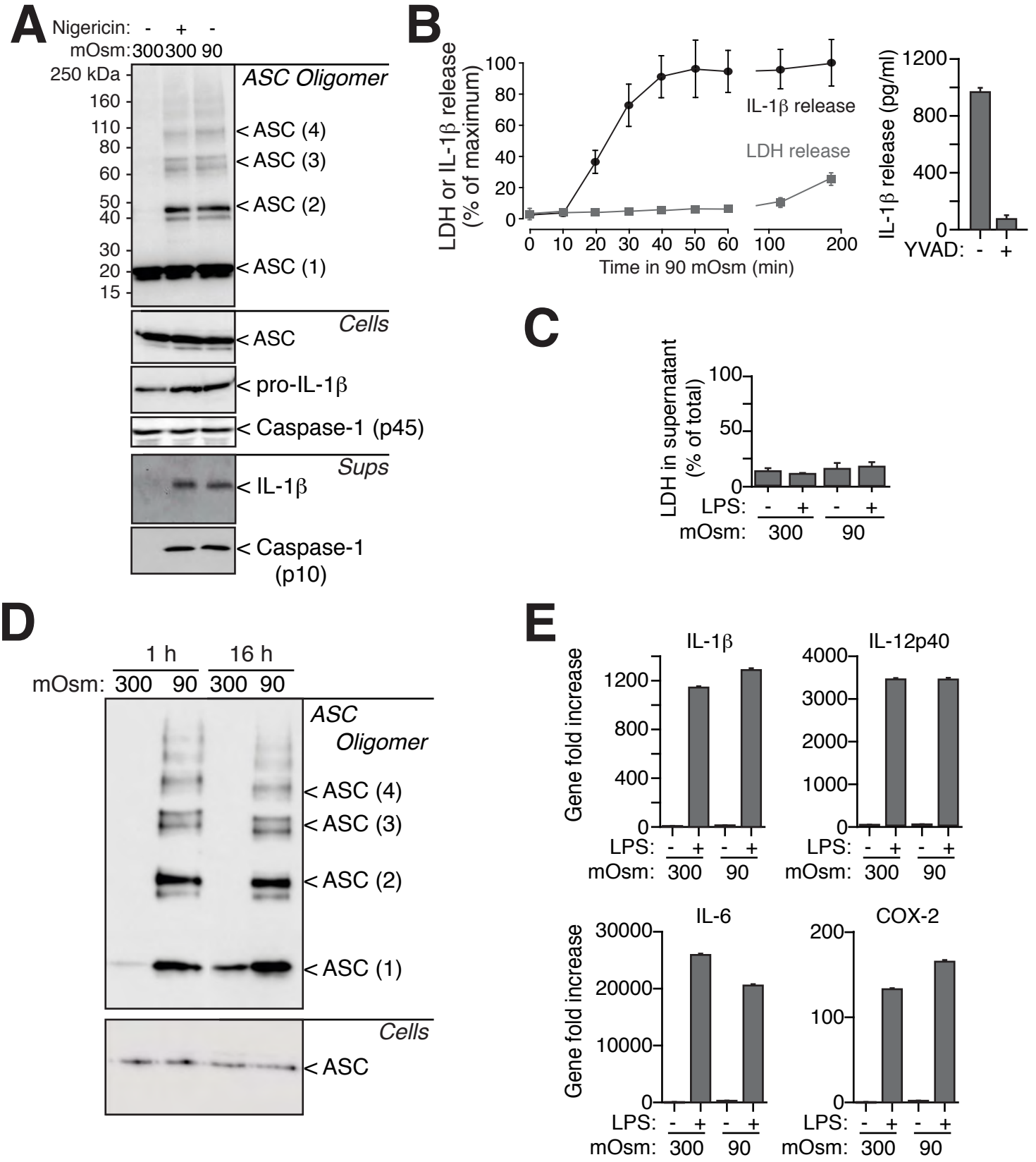
A
Nigericin: - + -
mOsm: 300 300 90
250 kDa
160
110
80
60
50
40
30
20
15
ASC Oligomer
< ASC (4)
< ASC (3)
< ASC (2)
< ASC (1)
Cells
< ASC
< pro-IL-1β
< Caspase-1 (p45)
Sups
< IL-1β
< Caspase-1 (p10)
B
LDH or IL-1β release (% of maximum)
IL-1β release
LDH release
Time in 90 mOsm (min)
IL-1β release (pg/ml)
YVAD: - +
C
LDH in supernatant (% of total)
LPS: - + - +
mOsm: 300 90
D
1 h 16 h
mOsm: 300 90 300 90
ASC Oligomer
< ASC (4)
< ASC (3)
< ASC (2)
< ASC (1)
Cells
< ASC
E
IL-1β
IL-12p40
IL-6
COX-2
Gene fold increase
LPS: - + - +
mOsm: 300 90

Figure 2

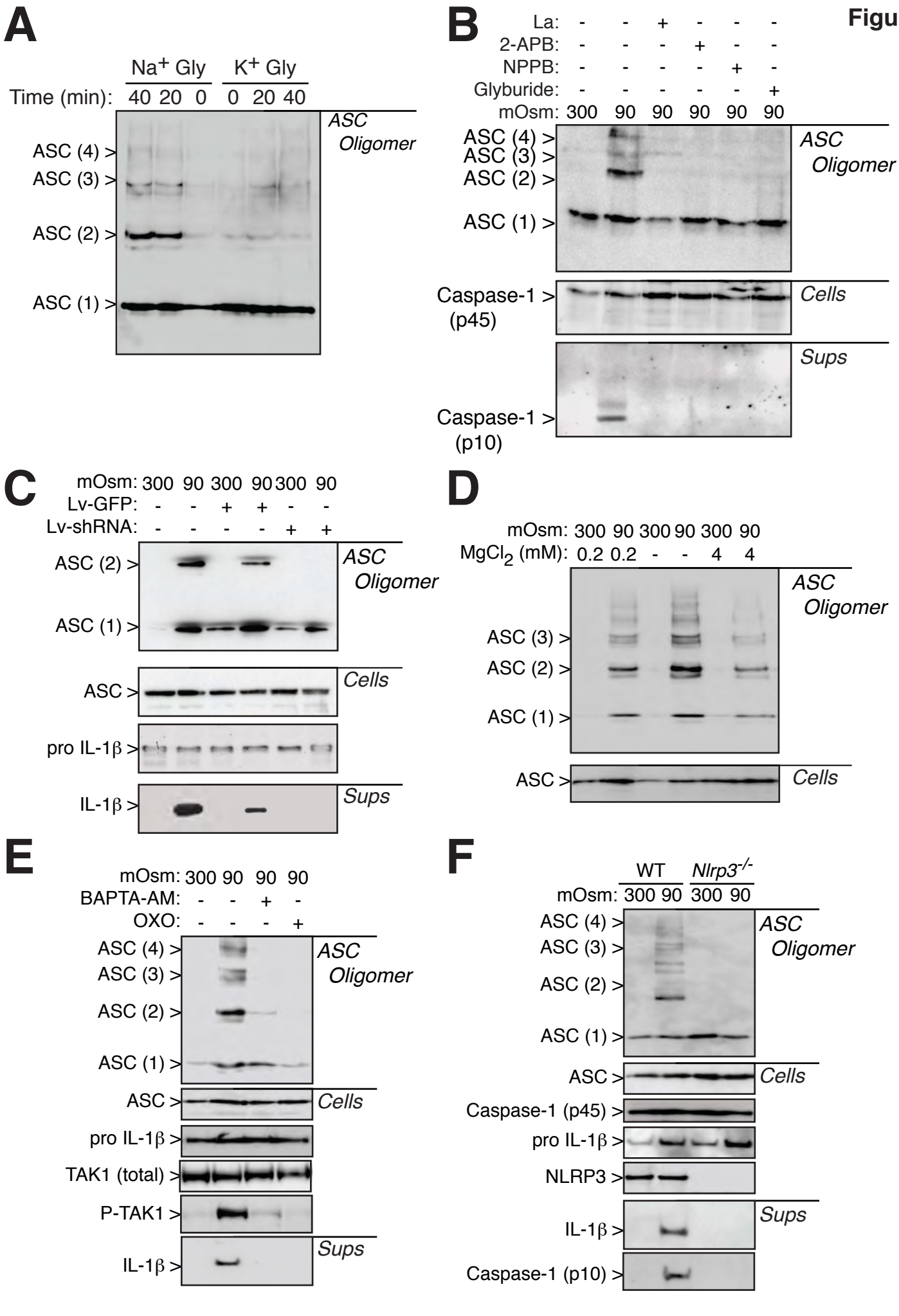
A
Na+ Gly
K+ Gly
Time (min): 40 20 0 0 20 40
ASC (4) >
ASC (3) >
ASC (2) >
ASC (1) >
ASC Oligomer
B
La: - - + - - -
2-APB: - - - + - -
NPPB: - - - - + -
Glyburide: - - - - - +
mOsm: 300 90 90 90 90 90
ASC (4) >
ASC (3) >
ASC (2) >
ASC (1) >
ASC Oligomer
Caspase-1 > (p45)
Cells
Sups
Caspase-1 > (p10)
C
mOsm: 300 90 300 90 300 90
Lv-GFP: - - + + - -
Lv-shRNA: - - - - + +
ASC (2) >
ASC (1) >
ASC Oligomer
ASC >
Cells
pro IL-1β >
IL-1β >
Sups
D
mOsm: 300 90 300 90 300 90
MgCl2 (mM): 0.2 0.2 - - 4 4
ASC (3) >
ASC (2) >
ASC (1) >
ASC Oligomer
ASC >
Cells
E
mOsm: 300 90 90 90
BAPTA-AM: - - + -
OXO: - - - +
ASC (4) >
ASC (3) >
ASC (2) >
ASC (1) >
ASC Oligomer
ASC >
Cells
pro IL-1β >
TAK1 (total) >
P-TAK1 >
IL-1β >
Sups
F
WT
Nlrp3-/-
mOsm: 300 90 300 90
ASC (4) >
ASC (3) >
ASC (2) >
ASC (1) >
ASC Oligomer
ASC >
Cells
Caspase-1 (p45) >
pro IL-1β >
NLRP3 >
IL-1β >
Sups
Caspase-1 (p10) >
Nlrp3-/-

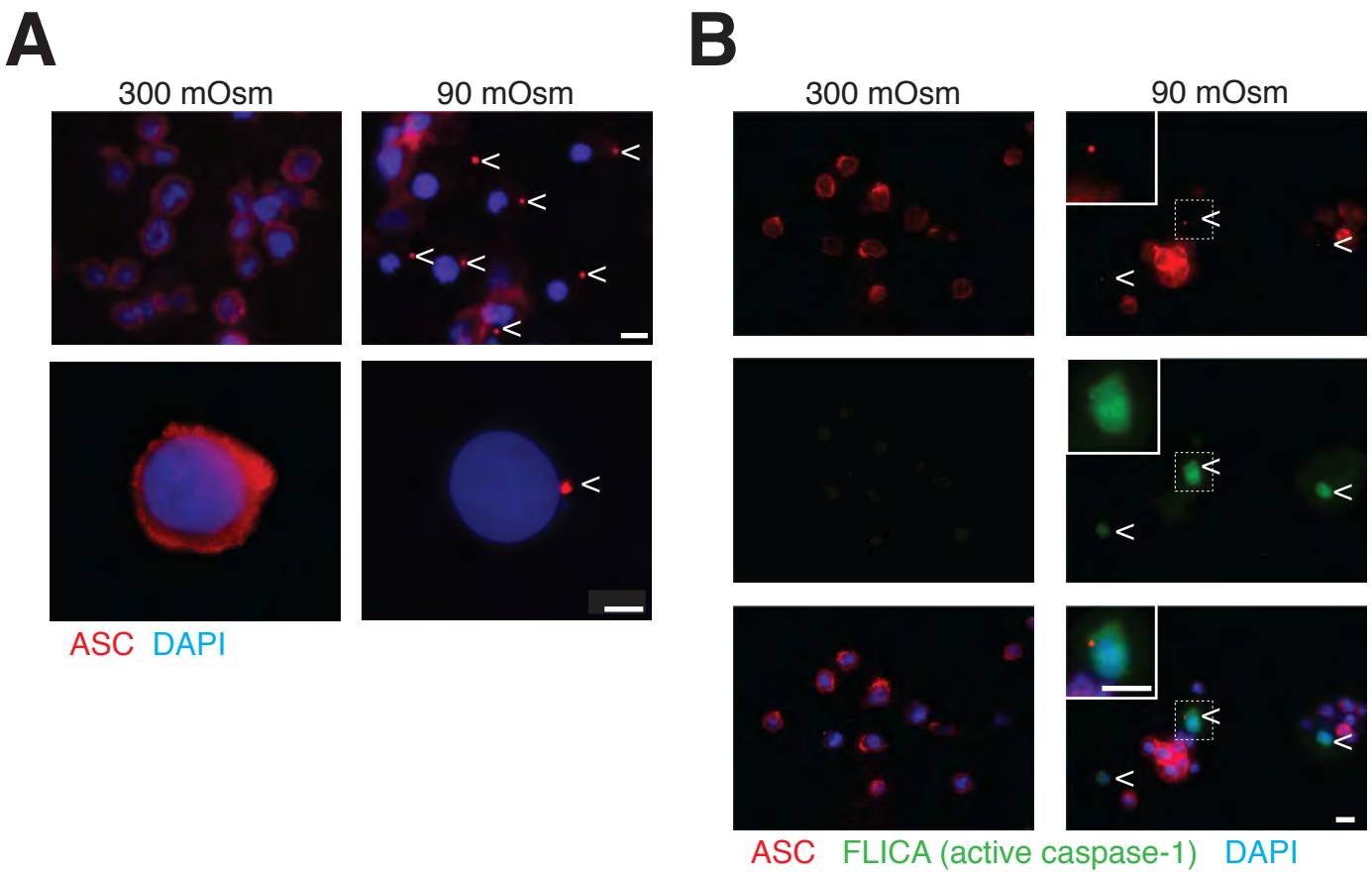
A
300 mOsm
90 mOsm
ASC DAPI
B
300 mOsm
90 mOsm
ASC FLICA (active caspase-1) DAPI

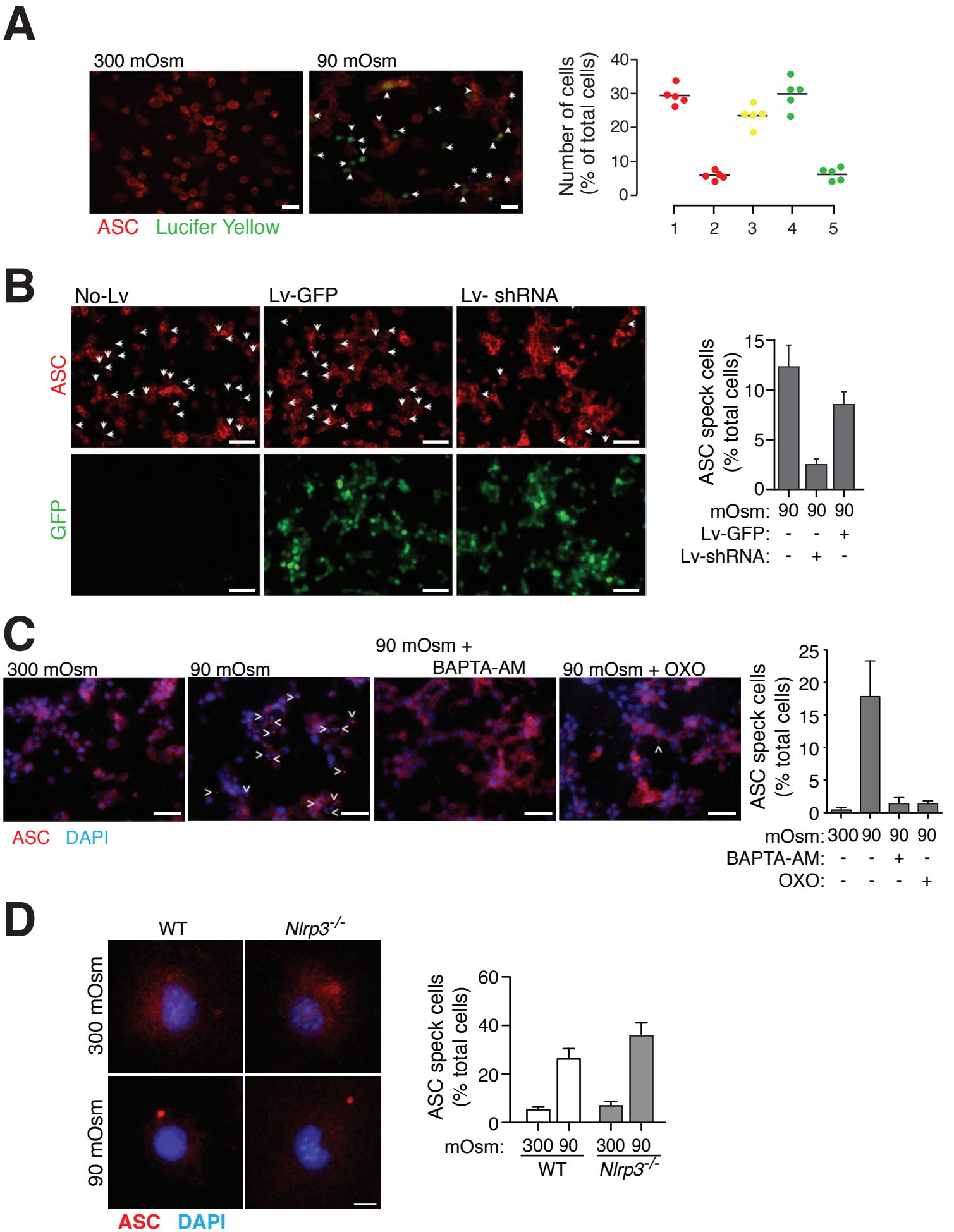
A
300 mOsm
90 mOsm
ASC Lucifer Yellow
Number of cells (% of total cells)
40
30
20
10
0
1 2 3 4 5
B
No-Lv
Lv-GFP
Lv- shRNA
ASC
GFP
ASC speck cells (% total cells)
15
10
5
0
mOsm: 90 90 90
Lv-GFP: - - +
Lv-shRNA: - + -
C
300 mOsm
90 mOsm
90 mOsm + BAPTA-AM
90 mOsm + OXO
ASC DAPI
ASC speck cells (% total cells)
25
20
15
10
5
0
mOsm: 300 90 90 90
BAPTA-AM: - - + -
OXO: - - - +
D
WT
Nlrp3-/-
300 mOsm
90 mOsm
ASC DAPI
ASC speck cells (% total cells)
60
40
20
0
mOsm: 300 90 300 90
WT
Nlrp3-/-

Figure 5

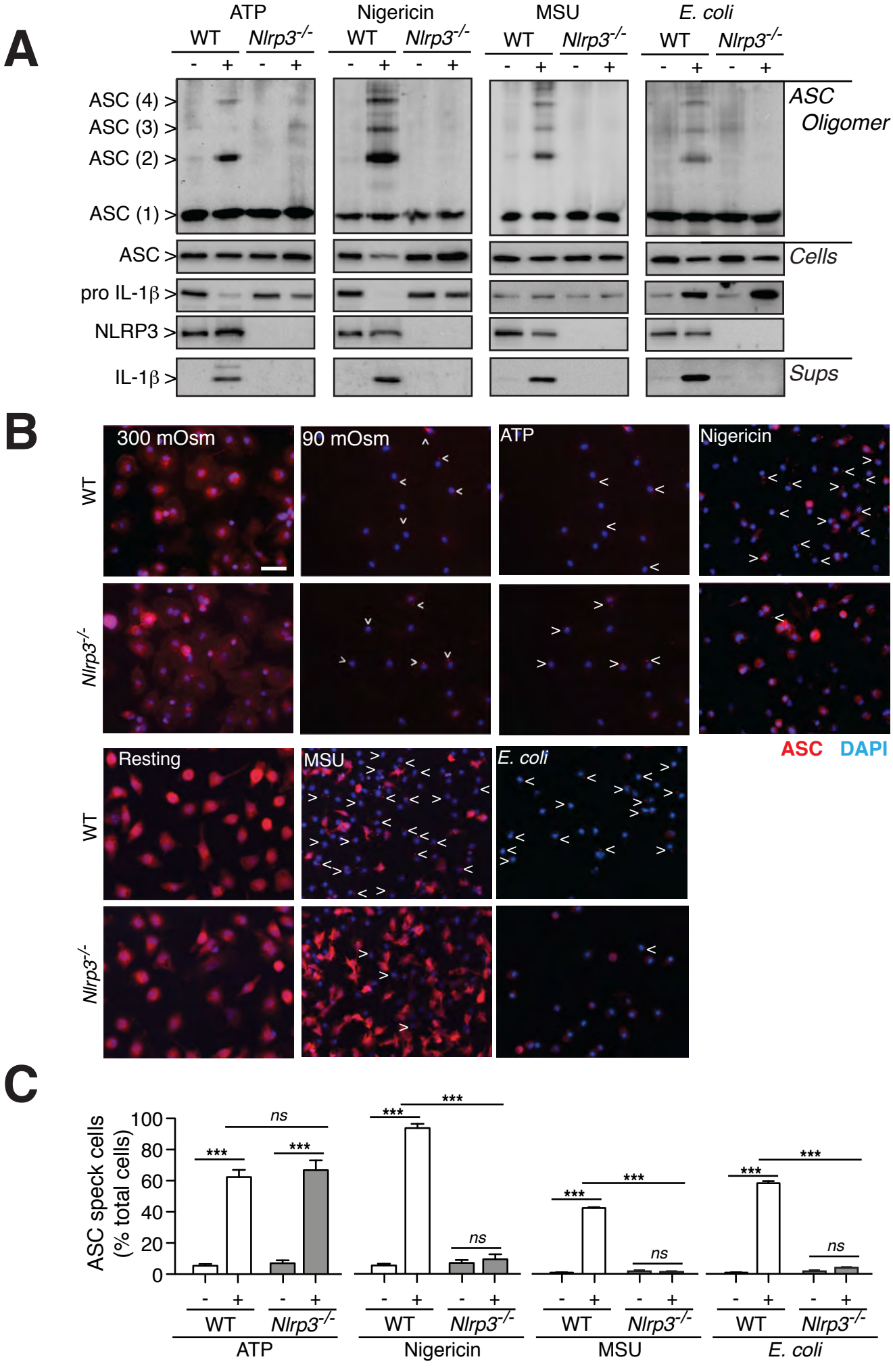
A
ATP
Nigericin
MSU
E. coli
WT
Nlrp3-/-
ASC (4)
ASC (3)
ASC (2)
ASC (1)
ASC Oligomer
ASC
Cells
pro IL-1β
NLRP3
IL-1β
Sups
B
300 mOsm
90 mOsm
ATP
Nigericin
Resting
MSU
E. coli
ASC DAPI
C
ASC speck cells (% total cells)
ns
***

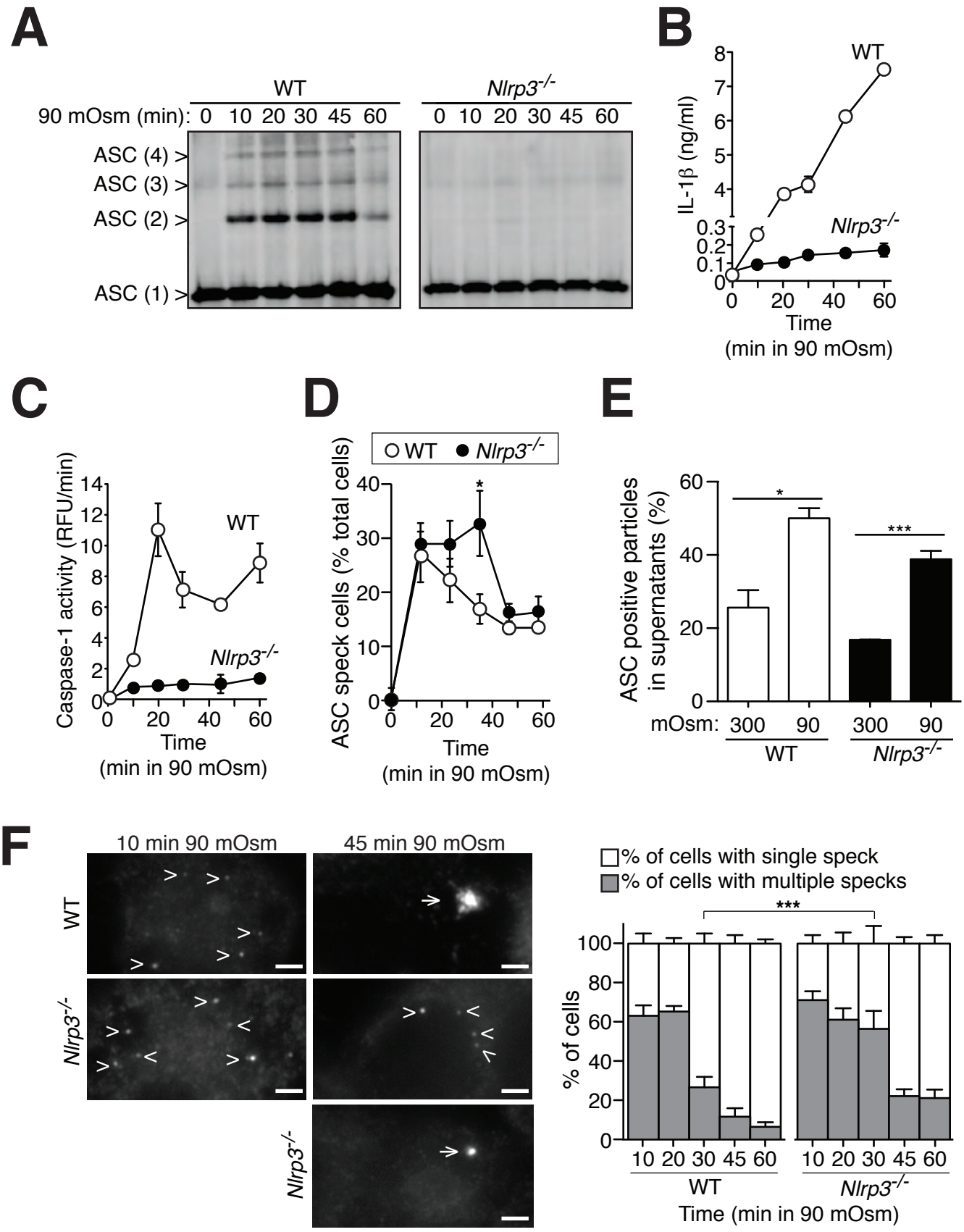
A
WT
Nlrp3-/-
90 mOsm (min): 0 10 20 30 45 60
0 10 20 30 45 60
ASC (4)
ASC (3)
ASC (2)
ASC (1)
B
WT
Nlrp3-/-
IL-1β (ng/ml)
Time
(min in 90 mOsm)
C
Caspase-1 activity (RFU/min)
WT
Nlrp3-/-
Time
(min in 90 mOsm)
D
WT
Nlrp3-/-
ASC speck cells (% total cells)
Time
(min in 90 mOsm)
E
ASC positive particles in supernatants (%)
mOsm: 300 90 300 90
WT
Nlrp3-/-
F
10 min 90 mOsm
45 min 90 mOsm
WT
Nlrp3-/-
Nlrp3-/-
% of cells with single speck
% of cells with multiple specks
% of cells
10 20 30 45 60 10 20 30 45 60
WT
Nlrp3-/-
Time (min in 90 mOsm)

Figure 7

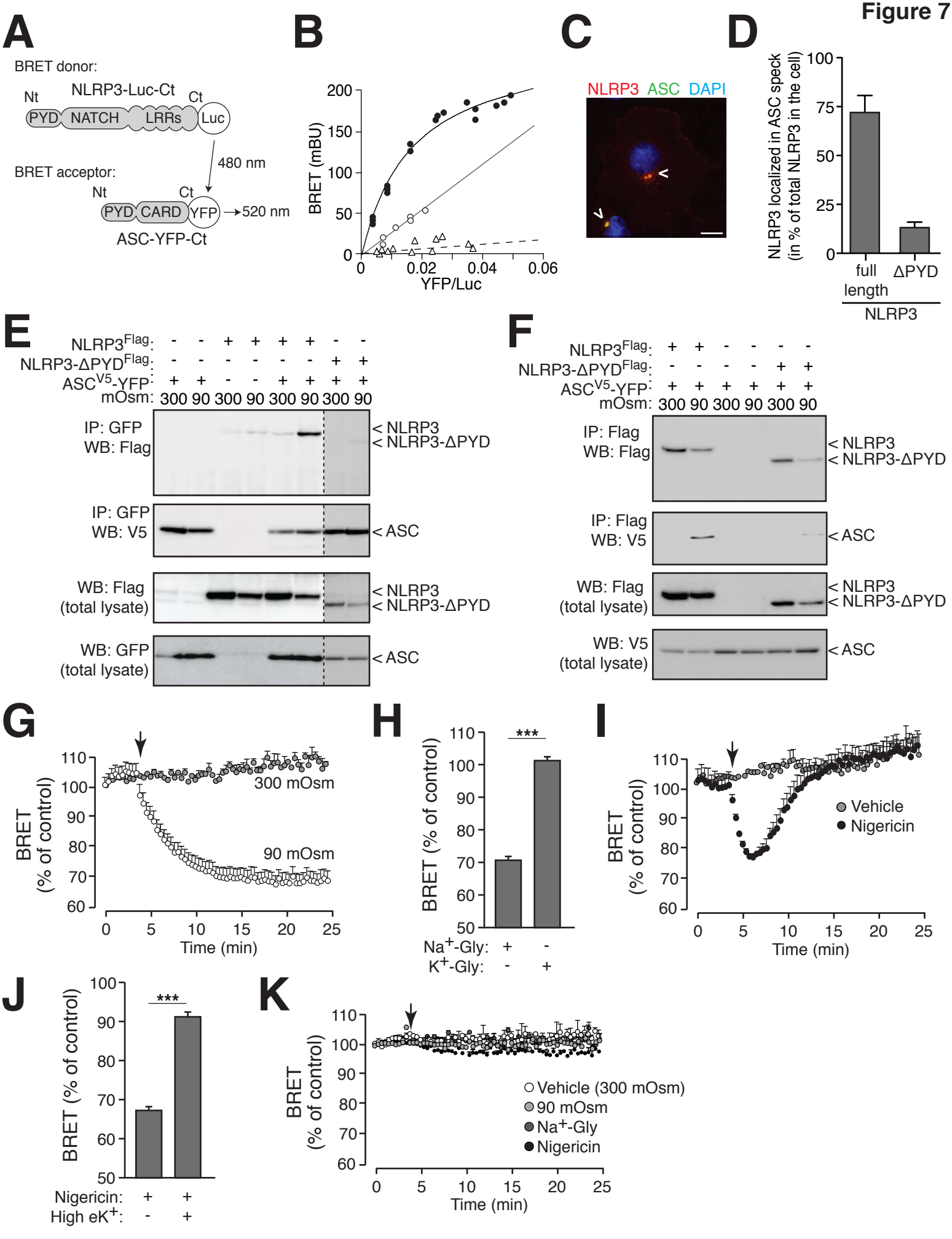
A
BRET donor:
Nt
NLRP3-Luc-Ct
Ct
PYD
NATCH
LRRs
Luc
480 nm
BRET acceptor:
Nt
Ct
PYD
CARD
YFP
520 nm
ASC-YFP-Ct
B
BRET (mBU)
YFP/Luc
C
NLRP3 ASC DAPI
D
NLRP3 localized in ASC speck (in % of total NLRP3 in the cell)
full length
ΔPYD
NLRP3
E
NLRP3Flag:
NLRP3-ΔPYDFlag:
ASCV5-YFP:
mOsm: 300 90 300 90 300 90 300 90
IP: GFP
WB: Flag
< NLRP3
< NLRP3-ΔPYD
IP: GFP
WB: V5
< ASC
WB: Flag
(total lysate)
< NLRP3
< NLRP3-ΔPYD
WB: GFP
(total lysate)
< ASC
F
NLRP3Flag:
NLRP3-ΔPYDFlag:
ASCV5-YFP:
mOsm: 300 90 300 90 300 90
IP: Flag
WB: Flag
< NLRP3
< NLRP3-ΔPYD
IP: Flag
WB: V5
< ASC
WB: Flag
(total lysate)
< NLRP3
< NLRP3-ΔPYD
WB: V5
(total lysate)
< ASC
G
BRET (% of control)
300 mOsm
90 mOsm
Time (min)
H
BRET (% of control)
***
Na+-Gly:
K+-Gly:
I
BRET (% of control)
Vehicle
Nigericin
Time (min)
J
BRET (% of control)
***
Nigericin:
High eK+:
K
BRET (% of control)
Vehicle (300 mOsm)
90 mOsm
Na+-Gly
Nigericin
Time (min)

Figure 8

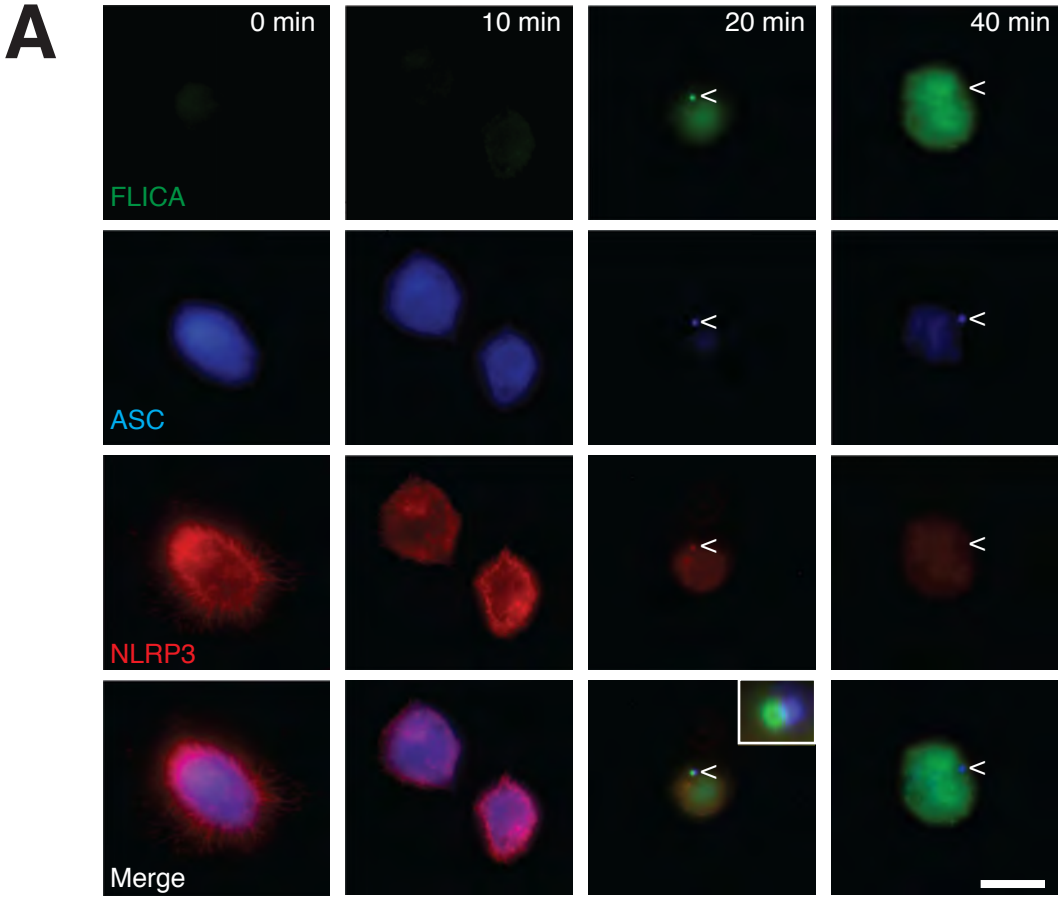
A
0 min
10 min
20 min
40 min
FLICA
ASC
NLRP3
Merge

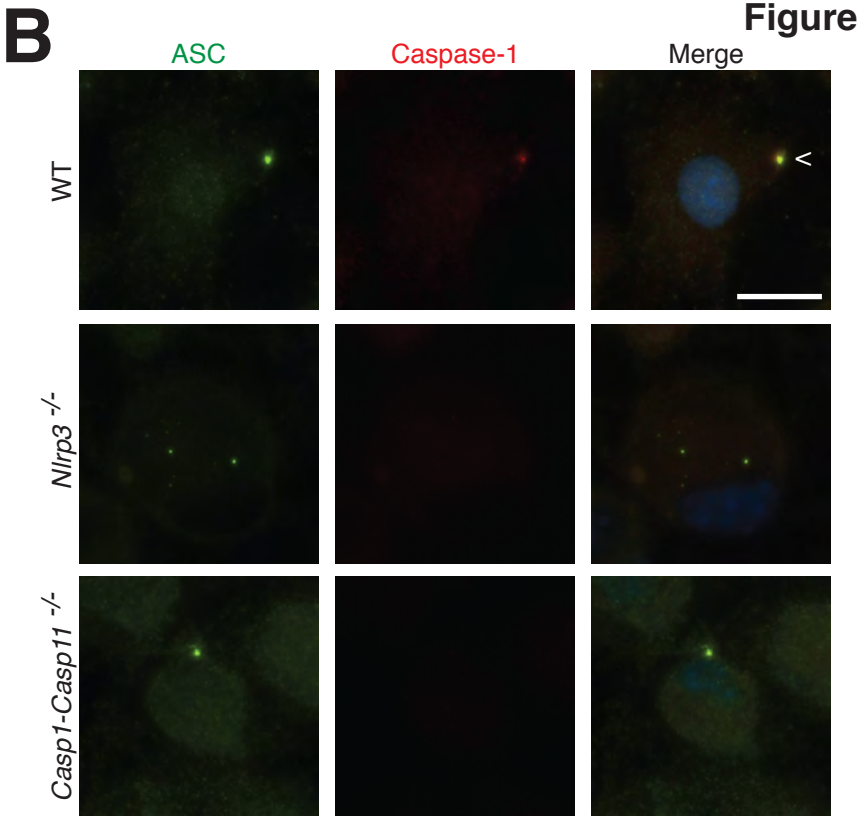
B
ASC
Caspase-1
Merge
WT
Nlrp3 -/-
Casp1-Casp11 -/-

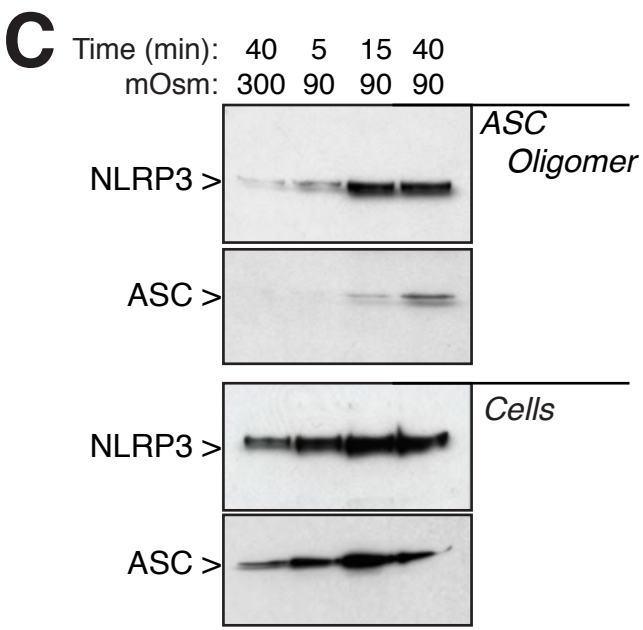
C
Time (min): 40 5 15 40
mOsm: 300 90 90 90
NLRP3 >
ASC >
ASC Oligomer
NLRP3 >
ASC >
Cells

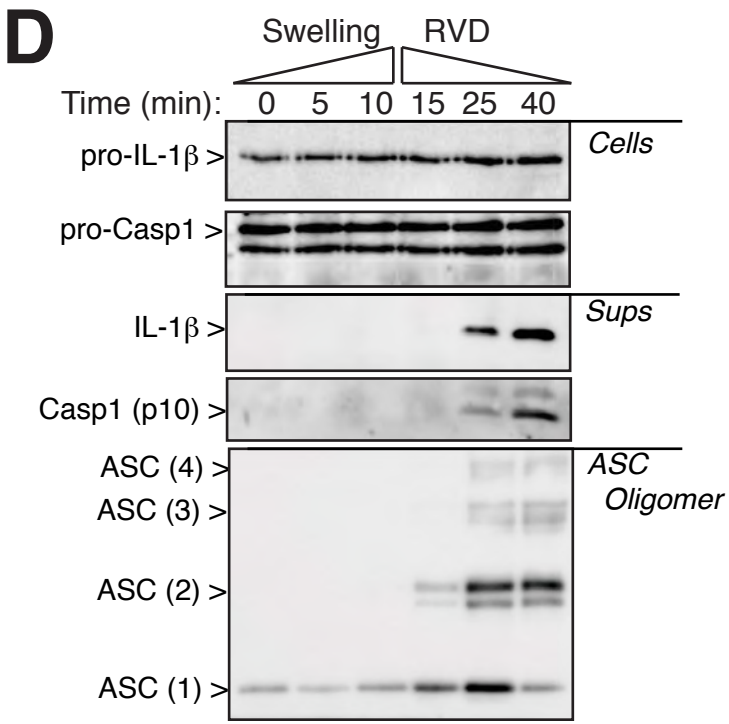
D
Swelling
RVD
Time (min): 0 5 10 15 25 40
pro-IL-1β >
pro-Casp1 >
Cells
IL-1β >
Casp1 (p10) >
Sups
ASC (4) >
ASC (3) >
ASC (2) >
ASC (1) >
ASC Oligomer